Responses to the Comments from the Associate Editor and the Reviewers

Dear Associate Editor and Reviewers,

We thank the Associate Editor for handling our submission and all the reviewers for providing us with valuable comments and suggestions to improve the quality of the paper. In this response letter, we summarize the changes made in the revised manuscript and then list the detailed responses to all the comments. To facilitate the verification of the revision, we have attached with this Response Letter a version with all the modifications highlighted in blue (with in red between brackets the associated reviewer and remarks numbers), except for some typo corrections.

Associate Editor's Comments

The two reviewers who evaluated the original version of the manuscript, scrutinised the revised version of the paper. One reviewer is entirely happy with the paper and has recommended that it be accepted. However, the first referee, while acknowledging that the article has improved, finds that there are some aspects of the paper which still need attention. These comments appear to be related to the way in which the authors' present their results and how they compare with other results in the literature. I suggest the authors look carefully at the comments of Referee 1 and prepare a revised version of their paper.

Response: Thank you very much for your comments and for providing us with a chance to improve our paper. In this new revision, we have carefully addressed all the comments of Referee 1. The modifications made in the revision are detailed below.

Comment 1: *In the last sentence of the first paragraph in section 1, it is said that the a posteriori analysis is required even for Lyapunov-based gain-scheduling controllers. Strictly speaking, this is not correct. The a posteriori analysis is necessary for only the following cases:*

1) *If the plant model and the practical systems have discrepancies.*
2) *If endogenous variables are used as the scheduling parameters.*

The reviewer thinks that appropriate revisions would help the possible reader to understand the contents correctly.

Response: This statement has been corrected based on reviewer's suggestion (please see the last sentence of the first paragraph in Section 1, in page 1).

Comment 2: *In page 2, at the end of the eighth line, ``must safe'' is to be ``must be safe''.*

Response: This typo has been corrected (page 2).

Comment 3: *Just before equ. (32), ``we can consider ... $D_c^{\mathcal C}(\theta_e)$'', the reviewer thinks that this sentence gives an assumption. Thus, it should be clearly mentioned* *that, in this paper, $C_c^{\mathcal C}(\theta_e)=0$ and $D_c^{\mathcal C}(\theta_e) \neq 0$ are supposed.*

Response: Actually, it is not an assumption. Indeed, in Subsection 3.2.3 we are looking for filters with which the enhanced velocity-based algorithm proposed in the paper works, i.e., to guarantee that equations (23) and (31) coincide. Furthermore, we are looking for a generic scheme, i.e., the equality between (23) and (31) must hold for any matrices $A_c^{\mathcal C}(\theta_e)$, …, $D_c^{\mathcal C}(\theta_e)$ involved in the LTI controller architecture (3) with suitable dimensions. Consequently, the equality must hold for any given arbitrary value of these matrices. That is why we consider in the development some very specific values for these matrices in order to derive the properties of the filters. In the revised version, these elements are put forward in a more explicit manner (please see the highlighted sentences in pages 19-20).

Comment 4: *In the middle of the last paragraph on page 23, ``As expected, a small value of the parameter τ significantly degrades the performance of the closed-loop system''. But, at least to the reviewer, it is not so apparent. In velocity algorithm, small value of τ is recommended to recover the original control performance. But, in the numerical simulations, the steady errors appear with small value of τ. It is strange from the above-mentioned fact. So, some explanations would help the possible readers.*

Response: This is because both implementations are based on a pseudo derivative scheme, resulting in noise amplification when the filtering parameter τ is too small. Based on reviewer's suggestion, this point has been further clarified in the new version (please see the paragraph below Fig. 6 in page 23).

We hope that the quality of the current version of our paper is adequate for publication.

To appear in the *International Journal of Control*
Vol. 00, No. 00, Month 20XX, 1–26

An Enhanced Velocity-Based Algorithm for Safe Implementations of Gain-Scheduled Controllers

(*Received 00 Month 20XX; accepted 00 Month 20XX*)

This paper presents an enhanced velocity-based algorithm to implement gain-scheduled controllers for nonlinear and parameter dependent systems. A new scheme including pre- and post-filtering is proposed with the assumption that the time-derivative of the controller inputs are not available for feedback control. It is shown that the proposed control structure can preserve the input-output properties of the linearized closed-loop system in the neighbourhood of each equilibrium point, avoiding the emergence of the so-called hidden coupling terms. Moreover, it is guaranteed that this implementation will not introduce unobservable or uncontrollable unstable modes and hence, the internal stability will not be affected. A case study dealing with the design of a pitch-axis missile autopilot is carried out and the numerical simulation results confirm the validity of the proposed approach.

Keywords: Enhanced velocity-based algorithm, Gain-scheduling, Hidden coupling terms

1. Introduction

Gain-scheduling techniques have been successfully used for the design and the implementation of a great variety of control systems ; the main reason being that gain-scheduling control allows leveraging the well-established linear system control techniques developed for decades (Leith, & Leithead, 2000a; Rugh, & Shamma, 2000). Basically, a classic point-to-point gain-scheduling design consists in first linearizing the nonlinear plant around a finite set of operating points capturing the system behavior over the operating domain. Then, for each operating point, a Linear Time Invariant (LTI) controller is designed to achieve stability and performance requirements of the linearized closed-loop system. Finally, the LTI controllers are interpolated *a posteriori* along with the operating point evolving with respect to scheduling signals, yielding a Linear Parameter Varying (LPV) controller (Lawrence, & Rugh, 1995; Rugh, 1991; Shamma, & Athans, 1990). Nevertheless, *ad hoc* interpolation methods do not provide any stability and performance guarantees for the closed-loop system except at the operating points used in the synthesis. To solve this problem, more elaborated interpolation strategies have been developed, aimed at guaranteeing that the underlying closed-loop LPV system is stable as long as the rate of variation of the operating point remains below a certain upper bound (Stilwell, & Rugh, 2000). Modern LPV approaches, such as Lyapunov-based design, can achieve a LPV controller with guaranteed closed-loop stability and adequate level of performance for a given predefined rate of variation of the scheduling variable (Biannic, & Apkarian, 1999; Naus, 2009; Vesel, & Ilka, 2013; Wu, Yang, Packard, & Becker, 1995). [Reviewer 1 - Remark 1] However, it is worth mentioning that when endogenous signals are used as scheduling parameters, the behavior of the closed-loop system with the original nonlinear plant still needs to be assessed *a posteriori*.

The present work addresses an issue related to the implementation of LPV gain-scheduled controllers obtained by either of the aforementioned techniques, which arises when endogenous system variables, such as system outputs or state variables, are used as scheduling signals. Specifically, in this case, the gain-scheduled controller is quasi-LPV (Rugh, & Shamma, 2000), exhibiting nonlinear dynamics. Consequently, a naive implementation of the nonlinear gain-scheduled controller on the original nonlinear system may lead to the occurrence of extra terms in the linearized dynamics, called *hidden coupling terms* (Rugh, & Shamma, 2000). The hidden coupling terms generally introduce a discrepancy between the controller dynamics used in the design and the actual dynamics of the implemented gain-scheduled controller. To handle such a mismatch, it is necessary to proceed to an adequate implementation of the nonlinear gain-scheduled controller such that the linearization of the nonlinear closed-loop dynamics exhibits the same input-output properties as the feedback of the linearized plant and the corresponding linear controller used in the synthesis process (Leith, & Leithead, 1998; Leith, 1999). Moreover, the implementation [Reviewer 1 - Remark 2] must be safe in the sense that it will preserve the internal stability property, i.e., it does not introduce any unobservable or uncontrollable unstable modes. However, much attention in the work reported in the literature is only devoted to the controller design. Consequently, an inadequate implementation of the gain-scheduled controller may induce severe performance deterioration or even destabilization of the closed-loop system once applied to the original nonlinear plant (Leith, and Leithead, 2000b; Rugh, & Shamma, 2000).

A solution to avoid such a pitfall is to integrate the hidden coupling terms issue in the control design process. Indeed, these terms can be cancelled by an appropriate choice of the controller architecture. The conditions for achieving this objective are given by a set of first-order partial differential equations (Lawrence, & Rugh, 1995; Nichols, Reichert, & Rugh, 1993; Rugh, & Shamma, 2000). One can also resort to the Dynamic Gain Scheduled (DSG) technique (Yang, Herrmann, Lowenberg, & Chen, 2010; Yang, Hammoudi, Herrmann, Lowenberg, & Chen, 2012, 2015). In this method, a gain-scheduling design is first applied (e.g, classic point-to-point gain-scheduling with *a posteriori* interpolation, self-scheduling, LPV design based on Linear and Bilinear Matrix Inequalities (LMIs and BMIs)) and then, the gains of the nonlinear gain-scheduled controller are computed via the resolution of a set of partial differential equations. However, these two aforementioned approaches generally lead to complex controller architectures. In sharp contrast, taking advantage of recently developed self-scheduling methods (Do Valle, Menegaldo, & Simões, 2014; Lhachemi, Saussié, & Zhu, 2015; Magni, Le Gorrec, & Chiappa, 1998; Saussié, Saydy, & Akhrif, 2008), another solution developed in (Lhachemi, Saussié, & Zhu, 2016a,b,c) incorporates explicitly the hidden coupling terms in the synthesis process and avoids to resort to complex controller architectures.

The above solutions for integrating the hidden coupling terms directly in the synthesis phase are at the expense of an increased complexity of the synthesis procedure and are not directly applicable to all the classic or modern gain-scheduling techniques. In this case, assuming that the time-derivative of the controller inputs are available for feedback control, one can resort to the velocity-based implementation (Kaminer, Pascoal, Khargonekar, & Coleman, 1995), which is a generic gain-scheduled controller implementation that allows avoiding the occurrence of the hidden coupling terms. However, as the time-derivative of the controller inputs are not readily available in most of the practical applications, it requires to invoke pseudo-derivations. This approach may fail since pseudo-derivation introduces an extra pole in the controller dynamics, interfering in the closed-loop system dynamics. Such an interference may not preserve the input-output properties and hence, it can induce performance degradation or even the destabilization of the closed-loop system. In this paper, an enhanced velocity-based implementation is developed to tackle the problems related to pseudo-derivations involved in the standard treatment. The main feature of the proposed approach is that it preserves both input-output properties and internal stability of the linearized closed-loop system in the neighbourhood of each equilibrium point. Consequently, it results in a safe implementation without introducing unobservable or uncontrollable unstable modes.

The rest of the paper is organized as follows. Various notations and problem statement are introduced in Section 2. Then, details of the proposed solution and the corresponding theoretical analysis are presented in Section 3. Finally, the efficiency of the proposed approach is demonstrated via a case study on the design of a benchmark pitch-axis missile autopilot in Section 4, followed by some concluding remarks in Section 5.

2. Problem settings

2.1 *System model*

In this paper, we deal with nonlinear systems of the following state-space form:

$$\mathcal{S} := \begin{cases} \dot{\boldsymbol{x}} = f(\boldsymbol{x}, \boldsymbol{u}, \boldsymbol{w}) \\ \boldsymbol{y} = h(\boldsymbol{x}, \boldsymbol{u}, \boldsymbol{w}) \end{cases} \tag{1}$$

where $\boldsymbol{x} \in \mathbb{R}^n$ is the state vector, $\boldsymbol{u} \in \mathbb{R}^m$ the control input vector, $\boldsymbol{w} \in \mathbb{R}^q$ the exogenous input vector and $\boldsymbol{y} \in \mathbb{R}^p$ the output vector. The vector field $f : \mathbb{R}^n \times \mathbb{R}^m \times \mathbb{R}^q \to \mathbb{R}^n$ represents the plant dynamics and the function $h : \mathbb{R}^n \times \mathbb{R}^m \times \mathbb{R}^q \to \mathbb{R}^p$ generates the system outputs. It is assumed that f and h are both of class $\mathcal{C}^1$.

This paper considers the tracking control problem of slow time-varying reference commands. In this setting, $\boldsymbol{r} \in \mathbb{R}^{p_1}$ denotes the reference signals to track. System output vector $\boldsymbol{y}$ can then be split as follows: $\boldsymbol{y} = \begin{bmatrix}\boldsymbol{y}_1^\top \ \boldsymbol{y}_2^\top\end{bmatrix}^\top$, where $\boldsymbol{y}_1 \in \mathbb{R}^{p_1}$ is the vector of output signals that must track the vector $\boldsymbol{r}$, $\boldsymbol{y}_2 \in \mathbb{R}^{p_2}$ gathers all extra signals available for feedback and $p_1 + p_2 = p$. Accordingly, we have $\boldsymbol{y}_1 = h_1(\boldsymbol{x}, \boldsymbol{u}, \boldsymbol{w})$ and $\boldsymbol{y}_2 = h_2(\boldsymbol{x}, \boldsymbol{u}, \boldsymbol{w})$. The exogenous input vector is also decomposed as follows: $\boldsymbol{w} = \begin{bmatrix}\boldsymbol{d}^\top \ \boldsymbol{w}_m^\top\end{bmatrix}^\top \in \mathbb{R}^q$, where $\boldsymbol{d} \in \mathbb{R}^{q_1}$ is the vector of non measurable disturbances (e.g., sensor noise), $\boldsymbol{w}_m \in \mathbb{R}^{q_2}$ is the vector of measurable exogenous signals (e.g, altitude, airspeed, dynamic pressure in an aeronautical context) and $q_1 + q_2 = q$.

As the control objective is to make the output signal $\boldsymbol{y}_1$ track the reference $\boldsymbol{r}$, we are interested in equilibrium points such that their trimmed values, respectively denoted $\boldsymbol{y}_{1,e}$ and $\boldsymbol{r}_e$, coincide. This requirement can be formulated as a constraint $\boldsymbol{y}_{1,e} = \boldsymbol{r}_e \in \Omega$, where Ω is an open subset of $\mathbb{R}^{p_1}$. Furthermore, we consider in this work small disturbances $\boldsymbol{d}$ around their zero nominal value, i.e., the disturbance trim condition is such that $\boldsymbol{d}_e = \boldsymbol{0}$. Consequently, the following set of equilibrium points is introduced:

$$\mathcal{E}_q := \left\{(\boldsymbol{x}_e, \boldsymbol{u}_e, \boldsymbol{w}_e) \, : \, f(\boldsymbol{x}_e, \boldsymbol{u}_e, \boldsymbol{w}_e) = \boldsymbol{0}, \, h_1(\boldsymbol{x}_e, \boldsymbol{u}_e, \boldsymbol{w}_e) = \boldsymbol{r}_e, \, \boldsymbol{d}_e = \boldsymbol{0}, \, \boldsymbol{r}_e \in \Omega\right\},$$

where $\boldsymbol{x}_e$, $\boldsymbol{u}_e$ and $\boldsymbol{w}_e$ denote, respectively, the trimmed values of the state vector $\boldsymbol{x}$, the input vector $\boldsymbol{u}$ and the exogenous input vector $\boldsymbol{w}$. We assume that $\mathcal{E}_q$ can be parametrized by a vector, called operating point, $\boldsymbol{\theta} \in \Theta$, where Θ is an open subset of $\mathbb{R}^s$. Accordingly, we assume that there exists a $\mathcal{C}^1$ bijective function $\mu : \Theta \to \mathcal{E}_q$ such that:

$$(\boldsymbol{x}_e, \boldsymbol{u}_e, \boldsymbol{w}_e) \in \mathcal{E}_q \Leftrightarrow \exists \boldsymbol{\theta}_e \in \Theta \, : \, (\boldsymbol{x}_e, \boldsymbol{u}_e, \boldsymbol{w}_e) = \mu(\boldsymbol{\theta}_e).$$

Furthermore, it is assumed that the operating point $\boldsymbol{\theta}_e$ depends uniquely on the measured system output $\boldsymbol{y}_e$ and on the measurable endogenous vector $\boldsymbol{w}_{m,e}$. Note that this assumption directly implies that for any admissible vectors $\boldsymbol{y}_e$ and $\boldsymbol{w}_{m,e}$, there should be one and only one pair $(\boldsymbol{x}_e, \boldsymbol{u}_e)$

such that for $(\boldsymbol{x}_e, \boldsymbol{u}_e, \boldsymbol{w}_e) \in \mathcal{E}_q$, $h(\boldsymbol{x}_e, \boldsymbol{u}_e, \boldsymbol{w}_e) = \boldsymbol{y}_e$. Consequently, we assume there exists a $\mathcal{C}^1$ bijective function $\nu : \mathcal{R} \to \Theta$, where

$$\mathcal{R} = \{(\boldsymbol{y}_e, \boldsymbol{w}_{m,e}) \,:\, h(\boldsymbol{x}_e, \boldsymbol{u}_e, \boldsymbol{w}_e) = \boldsymbol{y}_e,\ (\boldsymbol{x}_e, \boldsymbol{u}_e, \boldsymbol{w}_e) \in \mathcal{E}_q\},$$

such that:

$$(\boldsymbol{x}_e, \boldsymbol{u}_e, \boldsymbol{w}_e) = \mu(\boldsymbol{\theta}_e) \Leftrightarrow \boldsymbol{\theta}_e = \nu(\boldsymbol{y}_e, \boldsymbol{w}_{m,e})$$

For synthesis purposes, the system $\mathcal{S}$ is linearized at each operating point $\boldsymbol{\theta}_e \in \Theta$ (i.e., around the equilibrium point $\mu(\boldsymbol{\theta}_e)$). Denoting respectively by $\boldsymbol{\delta x}$, $\boldsymbol{\delta u}$, $\boldsymbol{\delta w}$ and $\boldsymbol{\delta y}$ the deviations of $\boldsymbol{x}$, $\boldsymbol{u}$, $\boldsymbol{w}$ and $\boldsymbol{y}$ from their equilibrium value $\boldsymbol{x}_e$, $\boldsymbol{u}_e$, $\boldsymbol{w}_e$ and $\boldsymbol{y}_e$, the linearization of $\mathcal{S}$ yields:

$$\mathcal{S}_l(\boldsymbol{\theta}_e) := \begin{cases} \boldsymbol{\delta \dot{x}} = \mathbf{A}^{\mathcal{S}}(\boldsymbol{\theta}_e)\boldsymbol{\delta x} + \mathbf{B}_u^{\mathcal{S}}(\boldsymbol{\theta}_e)\boldsymbol{\delta u} + \mathbf{B}_w^{\mathcal{S}}(\boldsymbol{\theta}_e)\boldsymbol{\delta w} \\ \boldsymbol{\delta y} = \mathbf{C}^{\mathcal{S}}(\boldsymbol{\theta}_e)\boldsymbol{\delta x} + \mathbf{D}_u^{\mathcal{S}}(\boldsymbol{\theta}_e)\boldsymbol{\delta u} + \mathbf{D}_w^{\mathcal{S}}(\boldsymbol{\theta}_e)\boldsymbol{\delta w} \end{cases} \tag{2}$$

where $\mathbf{A}^{\mathcal{S}}(\boldsymbol{\theta}), \ldots, \mathbf{D}_w^{\mathcal{S}}(\boldsymbol{\theta})$ are matrices of suitable dimensions. Thus, the family of linear models associated to the system $\mathcal{S}$ over the operating domain Θ, is defined as follows:

$$\mathcal{S}_l := \{\mathcal{S}_l(\boldsymbol{\theta}_e) \,:\, \boldsymbol{\theta}_e \in \Theta\}.$$

2.2 *Set of linear controllers*

In gain-scheduling design, the first objective is to synthesize for each linearized model $\mathcal{S}_l(\boldsymbol{\theta}_e) \in \mathcal{S}_l$ a linear controller $\mathcal{C}_l(\boldsymbol{\theta}_e)$. In this work, it is supposed that the synthesis of the gain-scheduled controller can be performed based on any gain-scheduling synthesis method, e.g., classic point-to-point synthesis or modern LPV synthesis methods.

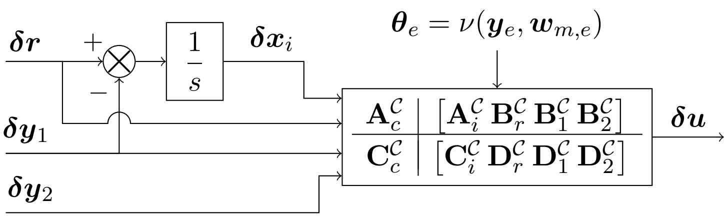

Figure 1. Linear controller $\mathcal{C}_l(\boldsymbol{\theta}_e)$

Let the signal $\boldsymbol{\delta r}$, $\boldsymbol{\delta y}_1$ and $\boldsymbol{\delta y}_2$ be respectively the deviations of $\boldsymbol{r}$, $\boldsymbol{y}_1$ and $\boldsymbol{y}_2$ from $\boldsymbol{r}_e$, $\boldsymbol{y}_{1,e}$ and $\boldsymbol{y}_{2,e}$. We consider a linear controller $\mathcal{C}_l(\boldsymbol{\theta}_e)$ of the following form (Fig. 1):

$$\mathcal{C}_l(\boldsymbol{\theta}_e) := \begin{cases} \boldsymbol{\delta \dot{x}}_i = \boldsymbol{\delta r} - \boldsymbol{\delta y}_1 \\ \boldsymbol{\delta \dot{x}}_c = \mathbf{A}_c^{\mathcal{C}}(\boldsymbol{\theta}_e)\boldsymbol{\delta x}_c + \mathbf{A}_i^{\mathcal{C}}(\boldsymbol{\theta}_e)\boldsymbol{\delta x}_i + \mathbf{B}_r^{\mathcal{C}}(\boldsymbol{\theta}_e)\boldsymbol{\delta r} + \mathbf{B}_1^{\mathcal{C}}(\boldsymbol{\theta}_e)\boldsymbol{\delta y}_1 + \mathbf{B}_2^{\mathcal{C}}(\boldsymbol{\theta}_e)\boldsymbol{\delta y}_2 \\ \boldsymbol{\delta u} = \mathbf{C}_c^{\mathcal{C}}(\boldsymbol{\theta}_e)\boldsymbol{\delta x}_c + \mathbf{C}_i^{\mathcal{C}}(\boldsymbol{\theta}_e)\boldsymbol{\delta x}_i + \mathbf{D}_r^{\mathcal{C}}(\boldsymbol{\theta}_e)\boldsymbol{\delta r} + \mathbf{D}_1^{\mathcal{C}}(\boldsymbol{\theta}_e)\boldsymbol{\delta y}_1 + \mathbf{D}_2^{\mathcal{C}}(\boldsymbol{\theta}_e)\boldsymbol{\delta y}_2 \end{cases} \tag{3}$$

where the controller state vector is composed of an integral component $\boldsymbol{\delta x}_i \in \mathbb{R}^{p_1}$, a vector $\boldsymbol{\delta x}_c \in \mathbb{R}^{n_c}$ and $\mathbf{A}_i^{\mathcal{C}}(\boldsymbol{\theta}), \ldots, \mathbf{D}_2^{\mathcal{C}}(\boldsymbol{\theta})$ are matrices of suitable dimensions with all the entries being $\mathcal{C}^1$ functions of the scheduling parameter $\boldsymbol{\theta} \in \Theta$. Then, the family of linear controllers over the operating domain

Θ is defined as follows:

$$\mathcal{C}_l := \{\mathcal{C}_l(\boldsymbol{\theta}_e) \,:\, \boldsymbol{\theta}_e \in \Theta\}\,.$$

In this framework, the design objective is to tune the gains of the fixed structure controller such that at each operating point $\boldsymbol{\theta}_e \in \Theta$, the closed-loop linear system (Fig. 2) composed of $\mathcal{S}_l(\boldsymbol{\theta}_e)$ and $\mathcal{C}_l(\boldsymbol{\theta}_e)$, denoted $\mathcal{CL}(\mathcal{S}_l(\boldsymbol{\theta}_e), \mathcal{C}_l(\boldsymbol{\theta}_e))$, is asymptotically stable and presents an appropriate level of performance. In the case of LPV control design, one may also guarantee both stability and performance of the closed-loop LPV system for a predefined rate of variation of the time-varying parameters.

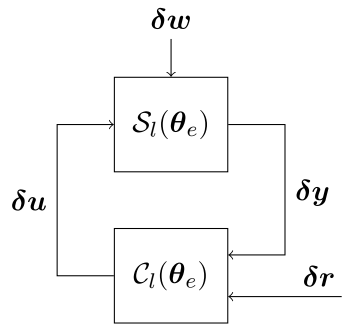

Figure 2. Closed-loop linear system $\mathcal{CL}(\mathcal{S}_l(\boldsymbol{\theta}_e), \mathcal{C}_l(\boldsymbol{\theta}_e))$

For the following developments, we introduce a state-space representation (4) of the linear controller $\mathcal{C}_l(\boldsymbol{\theta}_e)$ defined in (3) with the controller state vector $\boldsymbol{X}_l^\top = \begin{bmatrix}\boldsymbol{\delta x}_i^\top & \boldsymbol{\delta x}_c^\top\end{bmatrix}^\top$, the controller input $\boldsymbol{U}_l^\top = \begin{bmatrix}\boldsymbol{\delta r}^\top & \boldsymbol{\delta y}_1^\top & \boldsymbol{\delta y}_2^\top\end{bmatrix}^\top$ and the controller output $\boldsymbol{Y}_l = \boldsymbol{\delta u}$. Note that for notational simplicity, the dependency of controller matrices over the operating point $\boldsymbol{\theta}_e$ has been omitted. Thus, the linearized dynamics of the controller can be expressed as:

$$\begin{cases} \dot{\boldsymbol{X}}_l = \boldsymbol{\mathcal{A}}_l \boldsymbol{X}_l + \boldsymbol{\mathcal{B}}_l \boldsymbol{U}_l \\ \boldsymbol{Y}_l = \boldsymbol{\mathcal{C}}_l \boldsymbol{X}_l + \boldsymbol{\mathcal{D}}_l \boldsymbol{U}_l \end{cases} \tag{4}$$

where

$$\boldsymbol{\mathcal{A}}_l = \begin{bmatrix} \mathbf{0} & \mathbf{0} \\ \mathbf{A}_i^{\mathcal{C}} & \mathbf{A}_c^{\mathcal{C}} \end{bmatrix}, \qquad \boldsymbol{\mathcal{B}}_l = \begin{bmatrix} \mathbf{I}_{p_1} & -\mathbf{I}_{p_1} & \mathbf{0} \\ \mathbf{B}_r^{\mathcal{C}} & \mathbf{B}_1^{\mathcal{C}} & \mathbf{B}_2^{\mathcal{C}} \end{bmatrix},$$

$$\boldsymbol{\mathcal{C}}_l = \begin{bmatrix} \mathbf{C}_i^{\mathcal{C}} & \mathbf{C}_c^{\mathcal{C}} \end{bmatrix}, \qquad \boldsymbol{\mathcal{D}}_l = \begin{bmatrix} \mathbf{D}_r^{\mathcal{C}} & \mathbf{D}_1^{\mathcal{C}} & \mathbf{D}_2^{\mathcal{C}} \end{bmatrix}.$$

2.3 *Problem statement*

In the remainder of the paper, we assume that for a given nonlinear system $\mathcal{S}$, a family $\mathcal{C}_l$ of LTI controllers with the structure given by (3) has been designed over the operating domain such that, at any operating point $\theta_e \in \Theta$, $\mathcal{CL}(\mathcal{S}_l(\boldsymbol{\theta}_e), \mathcal{C}_l(\boldsymbol{\theta}_e))$ is stable and presents an adequate level of performance. Again, such a family can be obtained by any method of choice (e.g., classic or modern gain-scheduling synthesis methods). The next step aims at finding a (nonlinear) gain-scheduled controller:

$$\mathcal{C} := \begin{cases} \dot{\boldsymbol{x}}_k = f_k(\boldsymbol{x}_k, \boldsymbol{y}, \boldsymbol{r}, \boldsymbol{\theta}) \\ \boldsymbol{u} = h_k(\boldsymbol{x}_k, \boldsymbol{y}, \boldsymbol{r}, \boldsymbol{\theta}) \\ \boldsymbol{\theta} = \nu(\boldsymbol{y}, \boldsymbol{w}_m) \end{cases} \tag{5}$$

that can preserve the input-output property of the linearized closed-loop systems. In other words, the objective is to find a nonlinear controller $\mathcal{C}$ such that, once placed in closed-loop with $\mathcal{S}$ and linearized in the vicinity of any operating point $\boldsymbol{\theta}_e \in \Theta$, the resulting dynamic model coincides with the one obtained during the synthesis phase based on the interconnection of $\mathcal{S}_l(\boldsymbol{\theta}_e)$ and $\mathcal{C}_l(\boldsymbol{\theta}_e)$. This is an essential property guaranteeing that the implementation can fully comply with the controller design. In particular, such an implementation allows avoiding the occurrence of the hidden coupling terms, which is the main source of performance degradation and instability once the controller is applied to the original nonlinear plant. In order to formulate this problem, let $\mathcal{CL}(\mathcal{S}_l(\boldsymbol{\theta}_e), \mathcal{C}_l(\boldsymbol{\theta}_e)) : (\boldsymbol{\delta r}, \boldsymbol{\delta w}) \to \boldsymbol{\delta y}$ be the closed-loop system corresponding to the interconnection of the linear system $\mathcal{S}_l(\boldsymbol{\theta}_e)$ and the linear controller $\mathcal{C}_l(\boldsymbol{\theta}_e)$. The corresponding transfer function is denoted by $T(\mathcal{S}_l(\boldsymbol{\theta}_e), \mathcal{C}_l(\boldsymbol{\theta}_e))$. The nonlinear closed-loop system corresponding to the interconnection of the nonlinear system $\mathcal{S}$ and the nonlinear controller $\mathcal{C}$ is denoted by $\mathcal{CL}(\mathcal{S}, \mathcal{C}) : (\boldsymbol{r}, \boldsymbol{w}) \to \boldsymbol{y}$. Let $\mathcal{CL}_l(\mathcal{S}, \mathcal{C})(\boldsymbol{\theta}_e)$ be the linearization of $\mathcal{CL}(\mathcal{S}, \mathcal{C})$ at the operating point $\boldsymbol{\theta}_e \in \Theta$ and $T_l(\mathcal{S}, \mathcal{C})(\boldsymbol{\theta}_e)$ be the corresponding transfer function. The (nonlinear) gain-scheduled controller implementation problem can be formulated as follows.

Problem 1. Safe implementation of the gain-scheduled controller: *Find a (nonlinear) gain-scheduled controller $\mathcal{C}$ such that for each operating point $\boldsymbol{\theta}_e \in \Theta$, the following properties hold:*

(1) the closed-loop transfer function $T_l(\mathcal{S}, \mathcal{C})(\boldsymbol{\theta}_e)$ coincides with $T(\mathcal{S}_l(\boldsymbol{\theta}_e), \mathcal{C}_l(\boldsymbol{\theta}_e))$;
(2) if $\mathcal{CL}(\mathcal{S}_l(\boldsymbol{\theta}_e), \mathcal{C}_l(\boldsymbol{\theta}_e))$ is internally stable (i.e., do not present any unobservable or uncontrollable unstable mode), then so is $\mathcal{CL}_l(\mathcal{S}, \mathcal{C})(\boldsymbol{\theta}_e)$.

In Problem 1, requirement (1) aims at finding a nonlinear gain-scheduled controller $\mathcal{C}$ that can preserve, once linearized in the vicinity of any operating point $\theta_e \in \Theta$, the linearized input-output properties of the closed-loop system $\mathcal{CL}(\mathcal{S}_l(\boldsymbol{\theta}_e), \mathcal{C}_l(\boldsymbol{\theta}_e))$. As the strategy for elaborating such a nonlinear controller $\mathcal{C}$ might introduce hidden modes, requirement (2) imposes that such hidden modes must be stable, in order to guarantee the internal stability of the closed-loop system.

If a nonlinear gain-scheduled controller $\mathcal{C}$ that solves Problem 1 can be found, the stability and the performance of the closed-loop nonlinear system depend significantly on the design of the LTI controllers $\mathcal{C}_l(\boldsymbol{\theta}_e)$. However, assuming that the set of LTI controllers $\mathcal{C}_l$ is designed such that for any operating point $\boldsymbol{\theta}_e \in \Theta$, $\mathcal{CL}(\mathcal{S}_l(\boldsymbol{\theta}_e), \mathcal{C}_l(\boldsymbol{\theta}_e))$ is internally stable, the stability of the resulting closed-loop nonlinear system $\mathcal{CL}(\mathcal{S}, \mathcal{C})$ can be guaranteed for slow time variations of the reference input $\boldsymbol{r}$ and the exogenous input $\boldsymbol{w}$ (Lawrence, D., & Rugh, 1990; Rugh, & Shamma, 2000).

2.4 *A motivating example*

Before presenting a solution to Problem 1, let us consider the following second-order nonlinear system (Khalil, & Grizzle, 1996):

$$\begin{cases} \dot{x}_1 = \tan x_1 + x_2 \\ \dot{x}_2 = x_1 + u \\ y = x_2 \end{cases} \tag{6}$$

where u and y are respectively the system input and output. It is assumed that the state variables x_1 and x_2 are all available for feedback. The objective is to make the system output y track the reference signal r.

2.4.1 *Controller synthesis*

The system equilibrium point such that $y_e = \theta_e \in \mathbb{R}$ is characterized by:

$$x_{1,e}(\theta_e) = -\tan^{-1}\theta_e, \quad x_{2,e}(\theta_e) = y_e(\theta_e) = \theta_e, \quad u_e(\theta_e) = \tan^{-1}\theta_e.$$

Then, the linearization of the system around this equilibrium point yields:

$$\begin{cases} \delta\dot{x}_1 = (1+\theta_e^2)\delta x_1 + \delta x_2 \\ \delta\dot{x}_2 = \delta x_1 + \delta u \\ \delta y = \delta x_2 \end{cases} \tag{7}$$

where δx_1, δx_2, δy and δu represent deviations of x_1, x_2, y and u from $x_{1,e}(\theta_e)$, $x_{2,e}(\theta_e)$, $y_e(\theta_e)$ and $u_e(\theta_e)$. Around a given operating point characterized by θ_e, the following linear controller has been proposed in (Khalil, & Grizzle, 1996):

$$\begin{cases} \delta\dot{x}_i = \delta r - \delta y \\ \delta u = k_i(\theta_e)\delta x_i + k_1(\theta_e)\delta x_1 + k_2(\theta_e)\delta x_2 \end{cases} \tag{8}$$

where δr denotes the deviation of the reference signal r from its equilibrium $r_e = \theta_e$ and with feedback gains:

$$k_i(\theta_e) = -\frac{1}{1+\theta_e^2}, \quad k_1(\theta_e) = -3 - (1+\theta_e^2)(3+\theta_e^2) - \frac{1}{1+\theta_e^2}, \quad k_2(\theta_e) = -3 - \theta_e^2.$$

Feedback gains $k_i(\theta_e)$, $k_1(\theta_e)$ and $k_2(\theta_e)$ have been designed so the closed-loop eigenvalues of system (7) are -1, $-1/2 \pm j\sqrt{3}/2$, for any $\theta_e \in \mathbb{R}$.

2.4.2 *Naive implementations*

A gain-scheduling scheme is required to implement controllers (8) along with the nonlinear system (6). A naive approach is to substitute δx_1, δx_2, δy and δu by $x_1 - x_{1,e}(y)$, $x_2 - x_{2,e}(y)$, $y - y_e(y)$ and $u - u_e(y)$ respectively, and replacing θ_e by y in (8). This implementation is not adequate because in this case δx_2 is replaced by $x_2 - x_{2,e}(y) = y - y = 0$, leading to the cancellation of the output feedback with gain k_2. Another naive approach is to implement the following nonlinear controller:

$$\begin{cases} \dot{x}_i = r - y \\ u = k_i(y)x_i + k_1(y)x_1 + k_2(y)y \end{cases} \tag{9}$$

Linearizing the controller dynamics yields

$$\begin{cases} \delta\dot{x}_i = \delta r - \delta y \\ \delta u = k_i^*(\theta_e)\delta x_i + k_1^*(\theta_e)\delta x_1 + k_2^*(\theta_e)\delta y \end{cases} \tag{10}$$

with $k_i^* = k_i$, $k_1^* = k_1$ and, denoting $x_{i,e}(\theta_e)$ the controller integral component trim condition,

$$\begin{aligned} k_2^*(\theta_e) &= k_2(\theta_e) + \left.\frac{\mathrm{d}k_i}{\mathrm{d}y}\right|_{\theta_e} x_{i,e}(\theta_e) + \left.\frac{\mathrm{d}k_1}{\mathrm{d}y}\right|_{\theta_e} x_{1,e}(\theta_e) + \left.\frac{\mathrm{d}k_2}{\mathrm{d}y}\right|_{\theta_e} \theta_e \\ &= k_2(\theta_e) - 4(1+\theta_e^2) + \frac{4}{1+\theta_e^2} + 2\left[\theta_e(7+3\theta_e^2) + \frac{2\theta_e}{1+\theta_e^2}\right]\tan^{-1}(\theta_e). \end{aligned}$$

Thus, the considered nonlinear controller (9) admits linearized dynamics (10) different from that given in (8) which is the one used in the design. Although scheduled gains have been selected in order to assign the closed-loop eigenvalues at -1, $-1/2 \pm j\sqrt{3}/2$ for all $\theta_e \in \mathbb{R}$, this is not the case for controller (9). In fact, with the naive approach, the closed-loop system is stable for $|\theta_e| < \theta_{\text{lim}}$ with $\theta_{\text{lim}} \approx 0.417$ and unstable otherwise. Obviously, such a naive implementation cannot preserve the input-output property of the linear closed-loop systems with linear controllers (8).

2.4.3 Velocity-based implementation

In order to preserve the input-output property of the linearized closed-loop systems with linear controllers (8), one may resort to the velocity-based implementation (Kaminer, Pascoal, Khargonekar, & Coleman, 1995). However, such an implementation requires the temporal derivative of the variables used for feedback, i.e., $\dot{r}$, $\dot{y}_1$ and $\dot{y}_2$, which are not readily available in most of the practical applications. To overcome this issue, it has been proposed in (Kaminer, Pascoal, Khargonekar, & Coleman, 1995) to employ pseudo-derivative of the inputs. Denoting by $\tau > 0$ the pseudo-derivative parameter, signals $\dot{r}$, $\dot{y}_1$ and $\dot{y}_2$ are estimated from r, y_1 and y_2 by resorting to the transfer function $s/(\tau s+1)$. The resulting implementation scheme for the set of LTI controllers $\mathcal{C}_l$ is given by (11), as illustrated in Fig. 3. Note that in Fig. 3, the transfer function $s/(\tau s + 1)$ has been split for comparison purposes with the subsequent implementation strategy proposed in Section 3.

$$\left\{ \begin{aligned} \dot{\boldsymbol{x}}_{r,f} &= -\tau^{-1}\boldsymbol{x}_{r,f} + \tau^{-1}\boldsymbol{r} \\ \dot{\boldsymbol{x}}_{y_1,f} &= -\tau^{-1}\boldsymbol{x}_{y_1,f} + \tau^{-1}\boldsymbol{y}_1 \\ \dot{\boldsymbol{x}}_{y_2,f} &= -\tau^{-1}\boldsymbol{x}_{y_2,f} + \tau^{-1}\boldsymbol{y}_2 \\ \dot{\boldsymbol{x}}_c &= \mathbf{A}_c(\boldsymbol{\theta})\boldsymbol{x}_c + \tau\mathbf{A}_i(\boldsymbol{\theta})[\boldsymbol{r} - \boldsymbol{y}_1] \\ &\quad + \mathbf{B}_r(\boldsymbol{\theta})[\boldsymbol{r} - \boldsymbol{x}_{r,f}] + \mathbf{B}_1(\boldsymbol{\theta})[\boldsymbol{y}_1 - \boldsymbol{x}_{y_1,f}] + \mathbf{B}_2(\boldsymbol{\theta})[\boldsymbol{y}_2 - \boldsymbol{x}_{y_2,f}] \\ \boldsymbol{v} &= \mathbf{C}_c(\boldsymbol{\theta})\boldsymbol{x}_c + \tau\mathbf{C}_i(\boldsymbol{\theta})[\boldsymbol{r} - \boldsymbol{y}_1] \\ &\quad + \mathbf{D}_r(\boldsymbol{\theta})[\boldsymbol{r} - \boldsymbol{x}_{r,f}] + \mathbf{D}_1(\boldsymbol{\theta})[\boldsymbol{y}_1 - \boldsymbol{x}_{y_1,f}] + \mathbf{D}_2(\boldsymbol{\theta})[\boldsymbol{y}_2 - \boldsymbol{x}_{y_2,f}] \\ \dot{\boldsymbol{u}} &= \tau^{-1}\boldsymbol{v} \\ \boldsymbol{\theta} &= \nu(\boldsymbol{y}, \boldsymbol{w}_m) \end{aligned} \right. \tag{11}$$

The application of the velocity-based implementation with pseudo-derivative of the inputs (11) to the motivating example leads to the following implementation of the family of LTI controllers given by (8):

$$\left\{ \begin{aligned} \dot{x}_{x_1,f} &= -\tau^{-1}x_{x_1,f} + \tau^{-1}x_1 \\ \dot{x}_{y,f} &= -\tau^{-1}x_{y,f} + \tau^{-1}y \\ v &= \tau k_i(y)(r-y) + k_1(y)(x_1 - x_{x_1,f}) + k_2(y)(y - x_{y,f}) \\ \dot{u} &= \tau^{-1}v \end{aligned} \right. \tag{12}$$

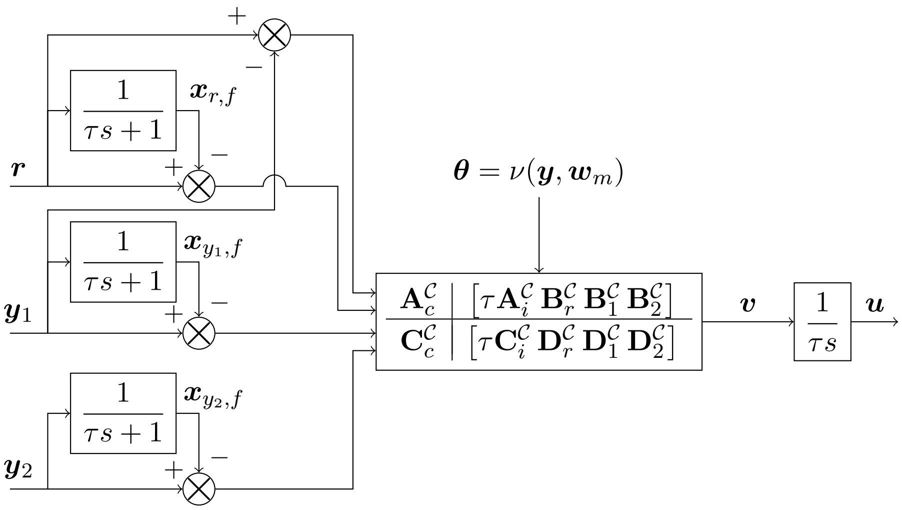

Figure 3. Velocity-based implementation with pseudo-derivative of the inputs

The linearization of this controller dynamics at the operating point θ_e yields in the Laplace domain:

$$\Delta u(s) = \frac{k_i(\theta_e)}{s}(\Delta r(s) - \Delta y(s)) + \frac{k_1(\theta_e)}{\tau s + 1}\Delta x_1(s) + \frac{k_2(\theta_e)}{\tau s + 1}\Delta y(s), \tag{13}$$

where $\Delta u(s)$, $\Delta r(s)$, $\Delta x_1(s)$ and $\Delta y(s)$ denote respectively the Laplace transforms of δu, δr, δx_1 and δy. Comparing (8) and (13) shows that the pseudo-derivative introduces an undesired pole in the linearized controller dynamics. It has been proven in (Kaminer, Pascoal, Khargonekar, & Coleman, 1995; Khalil, & Grizzle, 1996) that for any frozen operating point, the closed-loop system with this approximation recovers the nominal performances when τ tends to zero. However, there is no guarantee that this property holds uniformly over the operating domain. Hence, it may be impossible to find a suitable value of τ over the operating domain. For instance, based on the Routh Hurwitz criterion, a necessary condition for the closed-loop stability[1] with controller (12) is $\tau < 1/(1 + \theta_e^2)$. Therefore, it is impossible to find a unique $\tau > 0$ such that the closed-loop system is stable for all $\theta_e \in \mathbb{R}$. In practice, it may be sufficient to guarantee the stability over a compact operating domain, e.g., $|\theta_e| \leq \theta_{\text{lim}}$. Even in this case, practical difficulties arise when τ is too close to zero, because the pseudo derivative amounts to implementing a first order filter with a pole located in $-1/\tau$. For instance, at the operating point $\theta_e = 10$, the aforementioned necessary condition implies $\tau < 0.01$ for closed-loop stability.

3. Enhanced velocity-based implementation

In this section, assuming that the time-derivative of the controller inputs are not available for feedback control, we introduce an enhanced velocity-based implementation that preserves both input-output properties and internal stability of the linearized closed-loop system in the neighbourhood of each equilibrium point.

3.1 *Proposed strategy*

Given the set of linearized controllers $\mathcal{C}_l$, designed to stabilize the closed-loop system $\mathcal{CL}(\mathcal{S}_l(\boldsymbol{\theta}_e), \mathcal{C}_l(\boldsymbol{\theta}_e))$ at each operating point $\boldsymbol{\theta}_e \in \Theta$, the following gain-scheduled controller is pro-

[1]Note that this condition is necessary but not sufficient to guarantee the closed-loop stability.

posed for $\tau > 0$, as illustrated in Fig. 4:

$$\mathcal{C} := \begin{cases} \dot{\boldsymbol{x}}_{r,f} = -\tau^{-1}\boldsymbol{x}_{r,f} + \tau^{-1}\boldsymbol{r} \\ \dot{\boldsymbol{x}}_{y_1,f} = -\tau^{-1}\boldsymbol{x}_{y_1,f} + \tau^{-1}\boldsymbol{y}_1 \\ \dot{\boldsymbol{x}}_{y_2,f} = -\tau^{-1}\boldsymbol{x}_{y_2,f} + \tau^{-1}\boldsymbol{y}_2 \\ \dot{\boldsymbol{x}}_c = \mathbf{A}_c^{\mathcal{C}}(\boldsymbol{\theta})\boldsymbol{x}_c + \tau\mathbf{A}_i^{\mathcal{C}}(\boldsymbol{\theta})[\boldsymbol{x}_{r,f} - \boldsymbol{x}_{y_1,f}] \\ \qquad + \mathbf{B}_r^{\mathcal{C}}(\boldsymbol{\theta})[\boldsymbol{r} - \boldsymbol{x}_{r,f}] + \mathbf{B}_1^{\mathcal{C}}(\boldsymbol{\theta})[\boldsymbol{y}_1 - \boldsymbol{x}_{y_1,f}] + \mathbf{B}_2^{\mathcal{C}}(\boldsymbol{\theta})[\boldsymbol{y}_2 - \boldsymbol{x}_{y_2,f}] \\ \boldsymbol{v} = \mathbf{C}_c^{\mathcal{C}}(\boldsymbol{\theta})\boldsymbol{x}_c + \tau\mathbf{C}_i^{\mathcal{C}}(\boldsymbol{\theta})[\boldsymbol{x}_{r,f} - \boldsymbol{x}_{y_1,f}] \\ \qquad + \mathbf{D}_r^{\mathcal{C}}(\boldsymbol{\theta})[\boldsymbol{r} - \boldsymbol{x}_{r,f}] + \mathbf{D}_1^{\mathcal{C}}(\boldsymbol{\theta})[\boldsymbol{y}_1 - \boldsymbol{x}_{y_1,f}] + \mathbf{D}_2^{\mathcal{C}}(\boldsymbol{\theta})[\boldsymbol{y}_2 - \boldsymbol{x}_{y_2,f}] \\ \dot{\boldsymbol{x}}_{v,f} = \tau^{-1}\boldsymbol{v} \\ \boldsymbol{u} = \boldsymbol{x}_{v,f} + \boldsymbol{v} \\ \boldsymbol{\theta} = \nu(\boldsymbol{y}, \boldsymbol{w}_m) \end{cases} \tag{14}$$

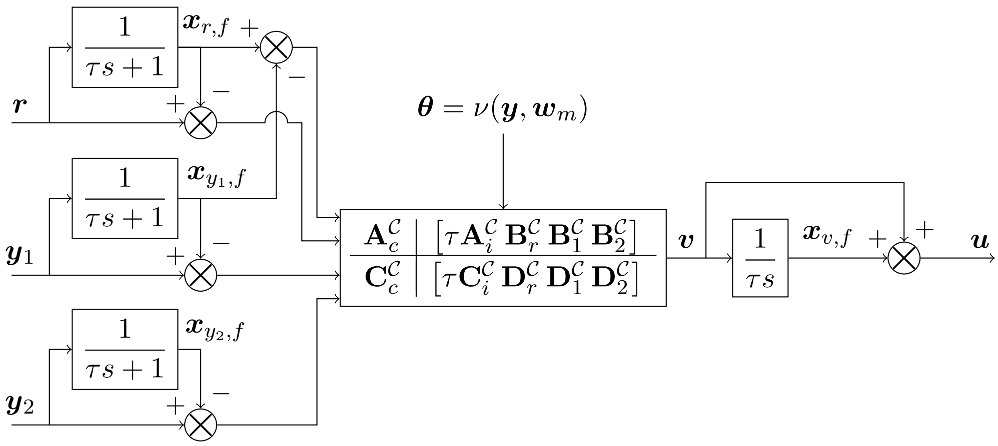

Figure 4. Enhanced velocity-based implementation

Note that for simplicity, the dependency of controller matrices over the operating point $\boldsymbol{\theta}$ has been omitted on Fig. 4. It can be observed that the proposed strategy presents a similar architecture to the velocity-based implementation with pseudo-derivative of the inputs (see Fig. 3). Indeed, the state-space matrices of the set of LTI controllers $\mathcal{C}_l$ are involved in an identical manner in these two strategies. Moreover, pre-filtering and an integral component at the controller output are also considered. However, as illustrated in the motivating example via the transfer function given in (13), the pseudo-derivative scheme with pre-filtering components introduces an undesired pole at $-1/\tau$. In order to cancel this harmful pole, the controller output, which was generated by an integral component with gain τ^{-1} (see Fig. 3), is augmented to also include a zero component located at $-1/\tau$. This can be observed on Fig. 4 because the transfer function between $\boldsymbol{v}$ and $\boldsymbol{u}$ is given by $(\tau s+1)/(\tau s)$. Finally, in the implementation shown in Fig. 3 the error signal $\boldsymbol{r} - \boldsymbol{y}_1$ is not pre-filtered. Thus, the post-filtering component introduces an uncompensated zero at $-1/\tau$. To avoid such a problem, the error signal is also pre-filtered in the proposed strategy. From the controller architecture $\mathcal{C}$, we can draw the following additional observations.

- Every controller input signal $\boldsymbol{z} \in \{\boldsymbol{r}, \boldsymbol{y}_1, \boldsymbol{y}_2\}$ is pre-filtered by a low-pass filter $1/(\tau s+1)$, resulting in signal $\boldsymbol{x}_{z,f}$. Thus, the error signal $\boldsymbol{z} - \boldsymbol{x}_{z,f}$, which is used for feedback, is composed of only medium and high frequencies components of the input signal $\boldsymbol{z}$. Note that for a signal $\boldsymbol{z}$ evolving around a frozen equilibrium value $\boldsymbol{z}_e$, one can expect that $\boldsymbol{x}_{z,f} \approx \boldsymbol{z}_e$, thus the error signal is such that $\boldsymbol{z} - \boldsymbol{x}_{z,f} \approx \boldsymbol{z} - \boldsymbol{z}_e$. This situation recovers the classic implementation of a linear controller around a given equilibrium point where only the deviations of the signal around the equilibrium point are used for feedback.

- The low frequency signal $\boldsymbol{x}_{r,f} - \boldsymbol{x}_{y_1,f}$ is also used in the feedback for tracking purposes. As detailed in the remainder of the paper, it is used to guarantee that in closed-loop the equilibrium condition $\boldsymbol{y}_{1,e} = \boldsymbol{r}_e$ is satisfied.
- The controller output is generated via post-filtering. At the equilibrium, one can find that the signal $\boldsymbol{v}$ generated by the controller is null in steady state, i.e., $\boldsymbol{v}_e = \mathbf{0}$. Therefore, the adequate controller output signal $\boldsymbol{u}$ in steady state $\boldsymbol{u}_e$ is generated by post-filtering via an integral component.
- The filtering parameter τ is involved in both $\boldsymbol{x}_c$-dynamics and $\boldsymbol{v}$-equation as a multiplying factor of both matrices $\mathbf{A}_i^{\mathcal{C}}(\boldsymbol{\theta})$ and $\mathbf{C}_i^{\mathcal{C}}(\boldsymbol{\theta})$. As demonstrated in the next subsection, this multiplying factor is required to preserve the input-output properties of the linearized closed-loop system.

3.2 *Properties of the enhanced velocity-based implementation*

In order to establish the properties of the enhanced velocity-based implementation, the following assumptions are made:

(A1) for any operating point $\boldsymbol{\theta}_e \in \Theta$, the matrix

$$\begin{bmatrix} \mathbf{A}_c^{\mathcal{C}}(\boldsymbol{\theta}_e) & \mathbf{A}_i^{\mathcal{C}}(\boldsymbol{\theta}_e) \\ \mathbf{C}_c^{\mathcal{C}}(\boldsymbol{\theta}_e) & \mathbf{C}_i^{\mathcal{C}}(\boldsymbol{\theta}_e) \end{bmatrix} \in \mathbb{R}^{(n_c+m)\times(n_c+p_1)} \tag{15}$$

is full column rank;

(A2) the dimension of the control input $\boldsymbol{u}$ coincides with the one of the reference signal $\boldsymbol{r}$, i.e, $m = p_1$;

(A3) for any operating point $\boldsymbol{\theta}_e \in \Theta$, the state-space representation of the linear controller $(\boldsymbol{\mathcal{A}}_l(\boldsymbol{\theta}_e), \boldsymbol{\mathcal{B}}_l(\boldsymbol{\theta}_e), \boldsymbol{\mathcal{C}}_l(\boldsymbol{\theta}_e), \boldsymbol{\mathcal{D}}_l(\boldsymbol{\theta}_e))$ introduced in (4) is stabilizable and detectable.

In particular, (A2) implies that for $\boldsymbol{\mathcal{C}}_l(\theta)$ the number of integrator channels coincides with the dimension of the reference signal $\boldsymbol{r}$. Assumption (A3) implies that all the hidden modes in controller dynamics correspond to stable poles.

3.2.1 Input-output properties

The main result of this section is the following theorem.

Theorem 1: *Suppose that (A1) holds and consider the nonlinear gain-scheduled controller $\mathcal{C}$ given in (14). Then, for any operating point $\boldsymbol{\theta}_e \in \Theta$, the closed-loop matrix transfer functions $T_l(\mathcal{S}, \mathcal{C})(\boldsymbol{\theta}_e)$ and $T(\mathcal{S}_l(\boldsymbol{\theta}_e), \mathcal{C}_l(\boldsymbol{\theta}_e))$ coincide.*

Proof: Let $\boldsymbol{\theta}_e \in \Theta$ be a given operating point. The equilibrium point of gain-scheduled controller

$\mathcal{C}$ is characterized by the following set of algebraic equations:

$$\begin{cases} \boldsymbol{x}_{r,f,e} = \boldsymbol{r}_e \\ \boldsymbol{x}_{y_1,f,e} = \boldsymbol{y}_{1,e} \\ \boldsymbol{x}_{y_2,f,e} = \boldsymbol{y}_{2,e} \\ \mathbf{0} = \mathbf{A}_c^{\mathcal{C}}(\boldsymbol{\theta}_e)\boldsymbol{x}_{c,e} + \tau\mathbf{A}_i^{\mathcal{C}}(\boldsymbol{\theta}_e)\left[\boldsymbol{r}_e - \boldsymbol{y}_{1,e}\right] \\ \mathbf{0} = \mathbf{C}_c^{\mathcal{C}}(\boldsymbol{\theta}_e)\boldsymbol{x}_{c,e} + \tau\mathbf{C}_i^{\mathcal{C}}(\boldsymbol{\theta}_e)\left[\boldsymbol{r}_e - \boldsymbol{y}_{1,e}\right] \\ \mathbf{0} = \boldsymbol{v}_e \\ \boldsymbol{u}_e = \boldsymbol{x}_{v,f,e} \end{cases} \tag{16}$$

In particular the fourth and fifth rows of the above system can be rewritten as follows:

$$\begin{bmatrix} \mathbf{A}_c^{\mathcal{C}}(\boldsymbol{\theta}_e) & \mathbf{A}_i^{\mathcal{C}}(\boldsymbol{\theta}_e) \\ \mathbf{C}_c^{\mathcal{C}}(\boldsymbol{\theta}_e) & \mathbf{C}_i^{\mathcal{C}}(\boldsymbol{\theta}_e) \end{bmatrix} \begin{bmatrix} \boldsymbol{x}_{c,e} \\ \tau\left[\boldsymbol{r}_e - \boldsymbol{y}_{1,e}\right] \end{bmatrix} = \mathbf{0}. \tag{17}$$

Based on (A1), it follows that $\boldsymbol{r}_e = \boldsymbol{y}_{1,e}$, $\boldsymbol{x}_{c,e} = \mathbf{0}$.

To prove that the matrix transfer functions $T_l(\mathcal{S},\mathcal{C})(\boldsymbol{\theta}_e)$ and $T(\mathcal{S}_l(\boldsymbol{\theta}_e),\mathcal{C}_l(\boldsymbol{\theta}_e))$ are equal, it is sufficient to show that the transfer function resulting from the linearization of the nonlinear gain-scheduled controller $\mathcal{C}$ at the operating point $\boldsymbol{\theta}_e$ coincides with the one resulting from $\mathcal{C}_l(\boldsymbol{\theta}_e)$ given in (3). To this end, the first step is to compute the linearization of controller $\mathcal{C}$ given by (14). For the given operating point $\boldsymbol{\theta}_e$, the deviation of the controller signals $\boldsymbol{x}_{r,f}$, $\boldsymbol{x}_{y_1,f}$, $\boldsymbol{x}_{y_2,f}$, $\boldsymbol{x}_c$, $\boldsymbol{v}$ and $\boldsymbol{x}_{v,f}$ from their equilibrium values specified above are denoted respectively by $\boldsymbol{\delta x}_{r,f}$, $\boldsymbol{\delta x}_{y_1,f}$, $\boldsymbol{\delta x}_{y_2,f}$, $\boldsymbol{\delta x}_c$, $\boldsymbol{\delta v}$ and $\boldsymbol{\delta x}_{v,f}$. The linarization of the pre-filter and the post-filter gives:

$$\begin{cases} \boldsymbol{\delta}\dot{\boldsymbol{x}}_{r,f} = -\tau^{-1}\boldsymbol{\delta x}_{r,f} + \tau^{-1}\boldsymbol{\delta r} \\ \boldsymbol{\delta}\dot{\boldsymbol{x}}_{y_1,f} = -\tau^{-1}\boldsymbol{\delta x}_{y_1,f} + \tau^{-1}\boldsymbol{\delta y}_1 \\ \boldsymbol{\delta}\dot{\boldsymbol{x}}_{y_2,f} = -\tau^{-1}\boldsymbol{\delta x}_{y_2,f} + \tau^{-1}\boldsymbol{\delta y}_2 \\ \boldsymbol{\delta}\dot{\boldsymbol{x}}_{v,f} = \tau^{-1}\boldsymbol{\delta v} \\ \boldsymbol{\delta u} = \boldsymbol{\delta x}_{v,f} + \boldsymbol{\delta v} \end{cases} \tag{18}$$

The linearization of the $\boldsymbol{x}_c$-dynamics and $\boldsymbol{v}$-equation, with $\boldsymbol{\theta} = \nu(\boldsymbol{y}, \boldsymbol{w}_m)$, is given by:

$$
\begin{aligned}
\boldsymbol{\delta}\dot{\boldsymbol{x}}_c =& \mathbf{A}_c^{\mathcal{C}}(\boldsymbol{\theta}_e)\boldsymbol{\delta x}_c + \frac{\partial}{\partial \boldsymbol{y}}\left[\mathbf{A}_c^{\mathcal{C}}(\boldsymbol{\theta})\boldsymbol{x}_c\right]\Big|_e \boldsymbol{\delta y} + \frac{\partial}{\partial \boldsymbol{w}_m}\left[\mathbf{A}_c^{\mathcal{C}}(\boldsymbol{\theta})\boldsymbol{x}_c\right]\Big|_e \boldsymbol{\delta w}_m \\
&+ \tau\mathbf{A}_i^{\mathcal{C}}(\boldsymbol{\theta}_e)[\boldsymbol{\delta x}_{r,f} - \boldsymbol{\delta x}_{y_1,f}] + \tau\,\frac{\partial}{\partial \boldsymbol{y}}\left[\mathbf{A}_i^{\mathcal{C}}(\boldsymbol{\theta})[\boldsymbol{x}_{r,f} - \boldsymbol{x}_{y_1,f}]\right]\Big|_e \boldsymbol{\delta y} \\
&+ \tau\,\frac{\partial}{\partial \boldsymbol{w}_m}\left[\mathbf{A}_i^{\mathcal{C}}(\boldsymbol{\theta})[\boldsymbol{x}_{r,f} - \boldsymbol{x}_{y_1,f}]\right]\Big|_e \boldsymbol{\delta w}_m \\
&+ \mathbf{B}_r^{\mathcal{C}}(\boldsymbol{\theta}_e)[\boldsymbol{\delta r} - \boldsymbol{\delta x}_{r,f}] + \frac{\partial}{\partial \boldsymbol{y}}\left[\mathbf{B}_r^{\mathcal{C}}(\boldsymbol{\theta})[\boldsymbol{r} - \boldsymbol{x}_{r,f}]\right]\Big|_e \boldsymbol{\delta y} \\
&+ \frac{\partial}{\partial \boldsymbol{w}_m}\left[\mathbf{B}_r^{\mathcal{C}}(\boldsymbol{\theta})[\boldsymbol{r} - \boldsymbol{x}_{r,f}]\right]\Big|_e \boldsymbol{\delta w}_m \\
&- \mathbf{B}_1^{\mathcal{C}}(\boldsymbol{\theta}_e)\boldsymbol{\delta x}_{y_1,f} + \frac{\partial}{\partial \boldsymbol{y}_1}\left[\mathbf{B}_1^{\mathcal{C}}(\boldsymbol{\theta})[\boldsymbol{y}_1 - \boldsymbol{x}_{y_1,f}]\right]\Big|_e \boldsymbol{\delta y}_1 \\
&+ \frac{\partial}{\partial \boldsymbol{y}_2}\left[\mathbf{B}_1^{\mathcal{C}}(\boldsymbol{\theta})[\boldsymbol{y}_1 - \boldsymbol{x}_{y_1,f}]\right]\Big|_e \boldsymbol{\delta y}_2 + \frac{\partial}{\partial \boldsymbol{w}_m}\left[\mathbf{B}_1^{\mathcal{C}}(\boldsymbol{\theta})[\boldsymbol{y}_1 - \boldsymbol{x}_{y_1,f}]\right]\Big|_e \boldsymbol{\delta w}_m \\
&- \mathbf{B}_2^{\mathcal{C}}(\boldsymbol{\theta}_e)\boldsymbol{\delta x}_{y_2,f} + \frac{\partial}{\partial \boldsymbol{y}_1}\left[\mathbf{B}_2^{\mathcal{C}}(\boldsymbol{\theta})[\boldsymbol{y}_2 - \boldsymbol{x}_{y_2,f}]\right]\Big|_e \boldsymbol{\delta y}_1 \\
&+ \frac{\partial}{\partial \boldsymbol{y}_2}\left[\mathbf{B}_2^{\mathcal{C}}(\boldsymbol{\theta})[\boldsymbol{y}_2 - \boldsymbol{x}_{y_2,f}]\right]\Big|_e \boldsymbol{\delta y}_2 + \frac{\partial}{\partial \boldsymbol{w}_m}\left[\mathbf{B}_2^{\mathcal{C}}(\boldsymbol{\theta})[\boldsymbol{y}_2 - \boldsymbol{x}_{y_2,f}]\right]\Big|_e \boldsymbol{\delta w}_m
\end{aligned}
\tag{19}
$$

$$
\begin{aligned}
\boldsymbol{\delta v} =& \mathbf{C}_c^{\mathcal{C}}(\boldsymbol{\theta}_e)\boldsymbol{\delta x}_c + \frac{\partial}{\partial \boldsymbol{y}}\left[\mathbf{C}_c^{\mathcal{C}}(\boldsymbol{\theta})\boldsymbol{x}_c\right]\Big|_e \boldsymbol{\delta y} + \frac{\partial}{\partial \boldsymbol{w}_m}\left[\mathbf{C}_c^{\mathcal{C}}(\boldsymbol{\theta})\boldsymbol{x}_c\right]\Big|_e \boldsymbol{\delta w}_m \\
&\tau\mathbf{C}_i^{\mathcal{C}}(\boldsymbol{\theta}_e)[\boldsymbol{\delta x}_{r,f} - \boldsymbol{\delta x}_{y_1,f}] + \tau\,\frac{\partial}{\partial \boldsymbol{y}}\left[\mathbf{C}_i^{\mathcal{C}}(\boldsymbol{\theta})[\boldsymbol{x}_{r,f} - \boldsymbol{x}_{y_1,f}]\right]\Big|_e \boldsymbol{\delta y} \\
&+ \tau\,\frac{\partial}{\partial \boldsymbol{w}_m}\left[\mathbf{C}_i^{\mathcal{C}}(\boldsymbol{\theta})[\boldsymbol{x}_{r,f} - \boldsymbol{x}_{y_1,f}]\right]\Big|_e \boldsymbol{\delta w}_m \\
&+ \mathbf{D}_r^{\mathcal{C}}(\boldsymbol{\theta}_e)[\boldsymbol{\delta r} - \boldsymbol{\delta x}_{r,f}] + \frac{\partial}{\partial \boldsymbol{y}}\left[\mathbf{D}_r^{\mathcal{C}}(\boldsymbol{\theta})[\boldsymbol{r} - \boldsymbol{x}_{r,f}]\right]\Big|_e \boldsymbol{\delta y} \\
&+ \frac{\partial}{\partial \boldsymbol{w}_m}\left[\mathbf{D}_r^{\mathcal{C}}(\boldsymbol{\theta})[\boldsymbol{r} - \boldsymbol{x}_{r,f}]\right]\Big|_e \boldsymbol{\delta w}_m \\
&- \mathbf{D}_1^{\mathcal{C}}(\boldsymbol{\theta}_e)\boldsymbol{\delta x}_{y_1,f} + \frac{\partial}{\partial \boldsymbol{y}_1}\left[\mathbf{D}_1^{\mathcal{C}}(\boldsymbol{\theta})[\boldsymbol{y}_1 - \boldsymbol{x}_{y_1,f}]\right]\Big|_e \boldsymbol{\delta y}_1 \\
&+ \frac{\partial}{\partial \boldsymbol{y}_2}\left[\mathbf{D}_1^{\mathcal{C}}(\boldsymbol{\theta})[\boldsymbol{y}_1 - \boldsymbol{x}_{y_1,f}]\right]\Big|_e \boldsymbol{\delta y}_2 + \frac{\partial}{\partial \boldsymbol{w}_m}\left[\mathbf{D}_1^{\mathcal{C}}(\boldsymbol{\theta})[\boldsymbol{y}_1 - \boldsymbol{x}_{y_1,f}]\right]\Big|_e \boldsymbol{\delta w}_m \\
&- \mathbf{D}_2^{\mathcal{C}}(\boldsymbol{\theta}_e)\boldsymbol{\delta x}_{y_2,f} + \frac{\partial}{\partial \boldsymbol{y}_1}\left[\mathbf{D}_2^{\mathcal{C}}(\boldsymbol{\theta})[\boldsymbol{y}_2 - \boldsymbol{x}_{y_2,f}]\right]\Big|_e \boldsymbol{\delta y}_1 \\
&+ \frac{\partial}{\partial \boldsymbol{y}_2}\left[\mathbf{D}_2^{\mathcal{C}}(\boldsymbol{\theta})[\boldsymbol{y}_2 - \boldsymbol{x}_{y_2,f}]\right]\Big|_e \boldsymbol{\delta y}_2 + \frac{\partial}{\partial \boldsymbol{w}_m}\left[\mathbf{D}_2^{\mathcal{C}}(\boldsymbol{\theta})[\boldsymbol{y}_2 - \boldsymbol{x}_{y_2,f}]\right]\Big|_e \boldsymbol{\delta w}_m
\end{aligned}
\tag{20}
$$

Note that the derivatives are evaluated at the equilibrium point characterized by the frozen operating point $\boldsymbol{\theta}_e$. In order to simplify (19) and (20), one can note that for $\boldsymbol{z} \in \{\boldsymbol{y}, \boldsymbol{w}_m\}$:

$$\frac{\partial}{\partial \boldsymbol{z}} \left[\mathbf{A}_c^{\mathcal{C}}(\boldsymbol{\theta})\boldsymbol{x}_c\right]\Big|_e = \sum_{k=1}^{n_c} x_{c,e}(k) \frac{\partial}{\partial \boldsymbol{z}} \left[\boldsymbol{A}_{c,C_k}^{\mathcal{C}}(\nu(\boldsymbol{y}, \boldsymbol{w}_m))\right]\Big|_e = \mathbf{0} \tag{21}$$

since $\boldsymbol{x}_{c,e} = \mathbf{0}$. In (21), $x_{c,e}(k)$ denotes the k-th element of vector $\boldsymbol{x}_{c,e}$ and $\boldsymbol{A}_{c,C_k}^{\mathcal{C}}$ denotes the k-th column of matrix $\mathbf{A}_c^{\mathcal{C}}$. Similarly, since $\boldsymbol{x}_{r,f,e} - \boldsymbol{x}_{y_1,f,e} = \mathbf{0}$, $\boldsymbol{x}_{c,e} = \mathbf{0}$, $\boldsymbol{r}_e - \boldsymbol{x}_{r,f,e} = \mathbf{0}$, $\boldsymbol{y}_{1,e} - \boldsymbol{x}_{y_1,f,e} = \mathbf{0}$, and $\boldsymbol{y}_{2,e} - \boldsymbol{x}_{y_2,f,e} = \mathbf{0}$, all the derivatives involved in (19) and (20) are equal to zero except $(\partial/\partial \boldsymbol{y}_1) \left[\mathbf{B}_1^{\mathcal{C}}(\boldsymbol{\theta})[\boldsymbol{y}_1 - \boldsymbol{x}_{y_1,f}]\right]\big|_e$, $(\partial/\partial \boldsymbol{y}_1) \left[\mathbf{D}_1^{\mathcal{C}}(\boldsymbol{\theta})[\boldsymbol{y}_1 - \boldsymbol{x}_{y_1,f}]\right]\big|_e$, $(\partial/\partial \boldsymbol{y}_2) \left[\mathbf{B}_2^{\mathcal{C}}(\boldsymbol{\theta})[\boldsymbol{y}_2 - \boldsymbol{x}_{y_2,f}]\right]\big|_e$ and $(\partial/\partial \boldsymbol{y}_2) \left[\mathbf{D}_2^{\mathcal{C}}(\boldsymbol{\theta})[\boldsymbol{y}_2 - \boldsymbol{x}_{y_2,f}]\right]\big|_e$. The first derivative becomes:

$$\begin{aligned}
&\frac{\partial}{\partial \boldsymbol{y}_1} \left[\mathbf{B}_1^{\mathcal{C}}(\boldsymbol{\theta})[\boldsymbol{y}_1 - \boldsymbol{x}_{y_1,f}]\right]\Big|_e \\
&= \frac{\partial}{\partial \boldsymbol{y}_1} \left[\sum_{k=1}^{p_1} [y_1(k) - x_{y_1,f}(k)] \boldsymbol{B}_{1,C_k}^{\mathcal{C}}(\nu(\boldsymbol{y}, \boldsymbol{w}_m))\right]\Bigg|_e \\
&= \sum_{k=1}^{p_1} \left\{ \frac{\partial}{\partial \boldsymbol{y}_1} \left[[y_1(k) - x_{y_1,f}(k)] \boldsymbol{B}_{1,C_k}^{\mathcal{C}}(\boldsymbol{\theta}_e)\right]\Big|_e + \underbrace{[y_{1,e}(k) - x_{y_1,f,e}(k)]}_{=0} \frac{\partial}{\partial \boldsymbol{y}_1} \left[\boldsymbol{B}_{1,C_k}^{\mathcal{C}}(\nu(\boldsymbol{y}, \boldsymbol{w}_m))\right]\Big|_e \right\} \\
&= \sum_{k=1}^{p_1} [\mathbf{0}| \dots |\mathbf{0}| \underbrace{\boldsymbol{B}_{1,C_k}^{\mathcal{C}}(\boldsymbol{\theta}_e)}_{k-\text{th column}} |\mathbf{0}| \dots |\mathbf{0}] \\
&= \mathbf{B}_1^{\mathcal{C}}(\boldsymbol{\theta}_e)
\end{aligned}$$

Similarly, the three other derivatives become $(\partial/\partial \boldsymbol{y}_1) \left[\mathbf{D}_1^{\mathcal{C}}(\boldsymbol{\theta})[\boldsymbol{y}_1 - \boldsymbol{x}_{y_1,f}]\right]\big|_e = \mathbf{D}_1^{\mathcal{C}}(\boldsymbol{\theta}_e)$, $(\partial/\partial \boldsymbol{y}_2) \left[\mathbf{B}_2^{\mathcal{C}}(\boldsymbol{\theta})[\boldsymbol{y}_2 - \boldsymbol{x}_{y_2,f}]\right]\big|_e = \mathbf{B}_2^{\mathcal{C}}(\boldsymbol{\theta}_e)$ and $(\partial/\partial \boldsymbol{y}_2) \left[\mathbf{D}_2^{\mathcal{C}}(\boldsymbol{\theta})[\boldsymbol{y}_2 - \boldsymbol{x}_{y_2,f}]\right]\big|_e = \mathbf{D}_2^{\mathcal{C}}(\boldsymbol{\theta}_e)$. Then, (19) and (20) can be simplified as:

$$\begin{cases}
\boldsymbol{\delta}\dot{\boldsymbol{x}}_c = \mathbf{A}_c^{\mathcal{C}}(\boldsymbol{\theta}_e)\boldsymbol{\delta x}_c + \tau \mathbf{A}_i^{\mathcal{C}}(\boldsymbol{\theta}_e)[\boldsymbol{\delta x}_{r,f} - \boldsymbol{\delta x}_{y_1,f}] + \mathbf{B}_r^{\mathcal{C}}(\boldsymbol{\theta}_e)[\boldsymbol{\delta r} - \boldsymbol{\delta x}_{r,f}] \\
\qquad + \mathbf{B}_1^{\mathcal{C}}(\boldsymbol{\theta}_e)[\boldsymbol{\delta y}_1 - \boldsymbol{\delta x}_{y_1,f}] + \mathbf{B}_2^{\mathcal{C}}(\boldsymbol{\theta}_e)[\boldsymbol{\delta y}_2 - \boldsymbol{\delta x}_{y_2,f}] \\
\boldsymbol{\delta v} = \mathbf{C}_c^{\mathcal{C}}(\boldsymbol{\theta}_e)\boldsymbol{\delta x}_c + \tau \mathbf{C}_i^{\mathcal{C}}(\boldsymbol{\theta}_e)[\boldsymbol{\delta x}_{r,f} - \boldsymbol{\delta x}_{y_1,f}] + \mathbf{D}_r^{\mathcal{C}}(\boldsymbol{\theta}_e)[\boldsymbol{\delta r} - \boldsymbol{\delta x}_{r,f}] \\
\qquad + \mathbf{D}_1^{\mathcal{C}}(\boldsymbol{\theta}_e)[\boldsymbol{\delta y}_1 - \boldsymbol{\delta x}_{y_1,f}] + \mathbf{D}_2^{\mathcal{C}}(\boldsymbol{\theta}_e)[\boldsymbol{\delta y}_2 - \boldsymbol{\delta x}_{y_2,f}]
\end{cases} \tag{22}$$

It is now straightforward to compute the transfer function of the linearized gain-scheduled controller dynamics at the operating point $\boldsymbol{\theta}_e$. First, based on (18), the transfer function of the pre-filter and the post-filter are given by:

$$\boldsymbol{\Delta x}_{r,f}(s) = \frac{1}{\tau s + 1}\boldsymbol{\Delta r}(s), \quad \boldsymbol{\Delta x}_{y_1,f}(s) = \frac{1}{\tau s + 1}\boldsymbol{\Delta y}_1(s),$$

$$\boldsymbol{\Delta x}_{y_2,f}(s) = \frac{1}{\tau s + 1}\boldsymbol{\Delta y}_2(s), \quad \boldsymbol{\Delta u}(s) = \frac{\tau s + 1}{\tau s}\boldsymbol{\Delta v}(s),$$

where $\boldsymbol{\Delta u}(s)$, $\boldsymbol{\Delta v}(s)$, $\boldsymbol{\Delta r}(s)$, $\boldsymbol{\Delta y_1}(s)$, $\boldsymbol{\Delta y_2}(s)$, $\boldsymbol{\Delta x}_{r,f}(s)$, $\boldsymbol{\Delta x}_{y_1,f}(s)$ and $\boldsymbol{\Delta x}_{y_2,f}(s)$ denote respectively the Laplace transforms of $\boldsymbol{\delta u}$, $\boldsymbol{\delta v}$, $\boldsymbol{\delta r}$, $\boldsymbol{\delta y}_1$, $\boldsymbol{\delta y}_2$, $\boldsymbol{\delta x}_{r,f}$, $\boldsymbol{\delta x}_{y_1,f}$ and $\boldsymbol{\delta x}_{y_2,f}$. Thus, it yields

$$\boldsymbol{\Delta r}(s) - \boldsymbol{\Delta x}_{r,f}(s) = \frac{\tau s}{\tau s+1}\boldsymbol{\Delta r}(s), \quad \boldsymbol{\Delta y}_1(s) - \boldsymbol{\Delta x}_{y_1,f}(s) = \frac{\tau s}{\tau s+1}\boldsymbol{\Delta y}_1(s),$$

$$\boldsymbol{\Delta y}_2(s) - \boldsymbol{\Delta x}_{y_2,f}(s) = \frac{\tau s}{\tau s+1}\boldsymbol{\Delta y}_2(s), \quad \boldsymbol{\Delta x}_{r,f}(s) - \boldsymbol{\Delta x}_{y_1,f}(s) = \frac{1}{\tau s+1}\left(\boldsymbol{\Delta r}(s) - \boldsymbol{\Delta y_1}(s)\right).$$

Finally, based on these transfer functions and by taking the Laplace transformation of (22), the linearized dynamics of the gain-scheduled controller $\mathcal{C}$ can be expressed by the following transfer function:

$$\begin{aligned}\boldsymbol{\Delta u}(s) =& \frac{1}{s}\left[\mathbf{C}_i^{\mathcal{C}}(\boldsymbol{\theta}_e) + \mathbf{C}_c^{\mathcal{C}}(\boldsymbol{\theta}_e)(s\mathbf{I_n} - \mathbf{A}_c^{\mathcal{C}}(\boldsymbol{\theta}_e))^{-1}\mathbf{A}_i^{\mathcal{C}}(\boldsymbol{\theta}_e)\right]\left(\boldsymbol{\Delta r}(s) - \boldsymbol{\Delta y_1}(s)\right) \\ &+ \left[\mathbf{D}_r^{\mathcal{C}}(\boldsymbol{\theta}_e) + \mathbf{C}_c^{\mathcal{C}}(\boldsymbol{\theta}_e)(s\mathbf{I}_n - \mathbf{A}_c^{\mathcal{C}}(\boldsymbol{\theta}_e))^{-1}\mathbf{B}_r^{\mathcal{C}}(\boldsymbol{\theta}_e)\right]\boldsymbol{\Delta r}(s) \\ &+ \left[\mathbf{D}_1^{\mathcal{C}}(\boldsymbol{\theta}_e) + \mathbf{C}_c^{\mathcal{C}}(\boldsymbol{\theta}_e)(s\mathbf{I_n} - \mathbf{A}_c^{\mathcal{C}}(\boldsymbol{\theta}_e))^{-1}\mathbf{B}_1^{\mathcal{C}}(\boldsymbol{\theta}_e)\right]\boldsymbol{\Delta y}_1(s) \\ &+ \left[\mathbf{D}_2^{\mathcal{C}}(\boldsymbol{\theta}_e) + \mathbf{C}_c^{\mathcal{C}}(\boldsymbol{\theta}_e)(s\mathbf{I_n} - \mathbf{A}_c^{\mathcal{C}}(\boldsymbol{\theta}_e))^{-1}\mathbf{B}_2^{\mathcal{C}}(\boldsymbol{\theta}_e)\right]\boldsymbol{\Delta y}_2(s)\end{aligned} \tag{23}$$

To conclude the proof, it is sufficient to note that, based on the linearized dynamics given by (3), the transfer function of $\mathcal{C}_l(\boldsymbol{\theta}_e)$ is identical to the one given by (23). $\square$

3.2.2 Internal stability

As shown in Theorem 1, the enhanced velocity-based implementation (14) can preserve the input-output properties of the set of linear controllers $\mathcal{C}_l$ since for any $\boldsymbol{\theta}_e \in \Theta$, $T_l(\mathcal{S},\mathcal{C})(\boldsymbol{\theta}_e) = T(\mathcal{S}_l(\boldsymbol{\theta}_e), \mathcal{C}_l(\boldsymbol{\theta}_e))$. However, it introduces a hidden mode as the pre-filtering pole $-1/\tau$ does not appear in the linearized controller dynamics transfer function. The presence of hidden modes requires the analysis of the internal stability of the closed-loop system. For this purpose, we consider the state-space representation of the linear controller $\mathcal{C}_l(\boldsymbol{\theta}_e)$ given in (4) and of the linearized dynamics of controller $\mathcal{C}$ which is, based on (18) and (22), given by:

$$\begin{cases}\dot{\boldsymbol{X}}_a = \boldsymbol{\mathcal{A}}_a\boldsymbol{X}_a + \boldsymbol{\mathcal{B}}_a\boldsymbol{U}_a \\ \boldsymbol{Y}_a = \boldsymbol{\mathcal{C}}_a\boldsymbol{X}_a + \boldsymbol{\mathcal{D}}_a\boldsymbol{U}_a\end{cases} \tag{24}$$

where $\boldsymbol{X}_a^\top = \left[\boldsymbol{\delta x}_{r,f}^\top\ \boldsymbol{\delta x}_{y_1,f}^\top\ \boldsymbol{\delta x}_{y_2,f}^\top\ \boldsymbol{\delta x}_c^\top\ \boldsymbol{\delta x}_{v,f}^\top\right]^\top$ is the controller state vector , $\boldsymbol{U}_a^\top = \left[\boldsymbol{\delta r}^\top\ \boldsymbol{\delta y}_1^\top\ \boldsymbol{\delta y}_2^\top\right]^\top$ the controller input, $\boldsymbol{Y}_a = \boldsymbol{\delta u}$ the controller output,

$$\boldsymbol{\mathcal{A}}_a = \begin{bmatrix} -\tau^{-1}\mathbf{I}_{p_1} & \mathbf{0} & \mathbf{0} & \mathbf{0} & \mathbf{0} \\ \mathbf{0} & -\tau^{-1}\mathbf{I}_{p_1} & \mathbf{0} & \mathbf{0} & \mathbf{0} \\ \mathbf{0} & \mathbf{0} & -\tau^{-1}\mathbf{I}_{p_2} & \mathbf{0} & \mathbf{0} \\ \tau\mathbf{A}_i^{\mathcal{C}} - \mathbf{B}_r^{\mathcal{C}} & -\tau\mathbf{A}_i^{\mathcal{C}} - \mathbf{B}_1^{\mathcal{C}} & -\mathbf{B}_2^{\mathcal{C}} & \mathbf{A}_c^{\mathcal{C}} & \mathbf{0} \\ \mathbf{C}_i^{\mathcal{C}} - \tau^{-1}\mathbf{D}_r^{\mathcal{C}} & -\mathbf{C}_i^{\mathcal{C}} - \tau^{-1}\mathbf{D}_1^{\mathcal{C}} & -\tau^{-1}\mathbf{D}_2^{\mathcal{C}} & \tau^{-1}\mathbf{C}_c^{\mathcal{C}} & \mathbf{0} \end{bmatrix},$$

$$\mathcal{B}_a = \begin{bmatrix} \tau^{-1}\mathbf{I}_{p_1} & \mathbf{0} & \mathbf{0} \\ \mathbf{0} & \tau^{-1}\mathbf{I}_{p_1} & \mathbf{0} \\ \mathbf{0} & \mathbf{0} & \tau^{-1}\mathbf{I}_{p_2} \\ \mathbf{B}_r^{\mathcal{C}} & \mathbf{B}_1^{\mathcal{C}} & \mathbf{B}_2^{\mathcal{C}} \\ \tau^{-1}\mathbf{D}_r^{\mathcal{C}} & \tau^{-1}\mathbf{D}_1^{\mathcal{C}} & \tau^{-1}\mathbf{D}_2^{\mathcal{C}} \end{bmatrix},$$

$$\boldsymbol{\mathcal{C}}_a = \begin{bmatrix} \tau\mathbf{C}_i^{\mathcal{C}} - \mathbf{D}_r^{\mathcal{C}} & -\tau\mathbf{C}_i^{\mathcal{C}} - \mathbf{D}_1^{\mathcal{C}} & -\mathbf{D}_2^{\mathcal{C}} & \mathbf{C}_c^{\mathcal{C}} & \mathbf{I}_m \end{bmatrix},$$

$$\boldsymbol{\mathcal{D}}_a = \begin{bmatrix} \mathbf{D}_r^{\mathcal{C}} & \mathbf{D}_1^{\mathcal{C}} & \mathbf{D}_2^{\mathcal{C}} \end{bmatrix}.$$

For notational simplicity, the dependency of the matrices in controller dynamics on operating point $\boldsymbol{\theta}_e$ is omitted. It is worth mentioning that the intermediate signal $\boldsymbol{v}$ involved in the gain-scheduled controller dynamics $\mathcal{C}$ given by (14) is neither a state variable nor a controller output. Therefore, it does not explicitly appear in the state-space model given by (24). However, the $\boldsymbol{\delta v}$-equation is considered for substituting $\boldsymbol{\delta v}$ into both $\boldsymbol{\delta x}_{v,f}$-dynamics and $\boldsymbol{\delta u}$-equation, which results in the state-space representation given in (24).

Lemma 1: *Assume that (A1) holds. For any $\lambda \in \mathbb{R}_+$, λ is an unobservable mode of $(\boldsymbol{\mathcal{A}}_a, \boldsymbol{\mathcal{C}}_a)$ if and only if it is an unobservable mode of $(\boldsymbol{\mathcal{A}}_l, \boldsymbol{\mathcal{C}}_l)$.*

Proof: Let $\boldsymbol{X} = \begin{bmatrix} \boldsymbol{x}_1^\top & \boldsymbol{x}_2^\top & \boldsymbol{x}_3^\top & \boldsymbol{x}_4^\top & \boldsymbol{x}_5^\top \end{bmatrix}^\top$ be a non zero vector with suitable dimensions such that $\boldsymbol{\mathcal{A}}_a\boldsymbol{X} = \lambda\boldsymbol{X}$ and $\boldsymbol{\mathcal{C}}_a\boldsymbol{X} = \mathbf{0}$. Then we have:

$$\begin{cases} -\dfrac{1}{\tau}\begin{bmatrix} \boldsymbol{x}_1 \\ \boldsymbol{x}_2 \\ \boldsymbol{x}_3 \end{bmatrix} = \lambda \begin{bmatrix} \boldsymbol{x}_1 \\ \boldsymbol{x}_2 \\ \boldsymbol{x}_3 \end{bmatrix} \\ (\tau\mathbf{A}_i^{\mathcal{C}} - \mathbf{B}_r^{\mathcal{C}})\boldsymbol{x}_1 + (-\tau\mathbf{A}_i^{\mathcal{C}} - \mathbf{B}_1^{\mathcal{C}})\boldsymbol{x}_2 - \mathbf{B}_2^{\mathcal{C}}\boldsymbol{x}_3 + \mathbf{A}_c^{\mathcal{C}}\boldsymbol{x}_4 = \lambda\boldsymbol{x}_4 \\ \left(\mathbf{C}_i^{\mathcal{C}} - \tau^{-1}\mathbf{D}_r^{\mathcal{C}}\right)\boldsymbol{x}_1 + \left(-\mathbf{C}_i^{\mathcal{C}} - \tau^{-1}\mathbf{D}_1^{\mathcal{C}}\right)\boldsymbol{x}_2 - \tau^{-1}\mathbf{D}_2^{\mathcal{C}}\boldsymbol{x}_3 + \tau^{-1}\mathbf{C}_c^{\mathcal{C}}\boldsymbol{x}_4 = \lambda\boldsymbol{x}_5 \\ (\tau\mathbf{C}_i^{\mathcal{C}} - \mathbf{D}_r^{\mathcal{C}})\boldsymbol{x}_1 + (-\tau\mathbf{C}_i^{\mathcal{C}} - \mathbf{D}_1^{\mathcal{C}})\boldsymbol{x}_2 - \mathbf{D}_2^{\mathcal{C}}\boldsymbol{x}_3 + \mathbf{C}_c^{\mathcal{C}}\boldsymbol{x}_4 + \boldsymbol{x}_5 = \mathbf{0} \end{cases} \tag{25}$$

As $\lambda \geq 0 > -1/\tau$, the first equations of (25) imply that $\boldsymbol{x}_1$, $\boldsymbol{x}_2$ and $\boldsymbol{x}_3$ are zero vectors. Then we have:

$$\begin{cases} \mathbf{A}_c^{\mathcal{C}}\boldsymbol{x}_4 = \lambda\boldsymbol{x}_4 \\ \tau^{-1}\mathbf{C}_c\boldsymbol{x}_4 = \lambda\boldsymbol{x}_5 \\ \mathbf{C}_c^{\mathcal{C}}\boldsymbol{x}_4 + \boldsymbol{x}_5 = \mathbf{0} \end{cases} \tag{26}$$

From the two last equations of (26), we obtain $(1/\tau + \lambda)\boldsymbol{x}_5 = \mathbf{0}$, which implies $\boldsymbol{x}_5 = \mathbf{0}$. Thus it yields:

$$\begin{cases} \mathbf{A}_c^{\mathcal{C}}\boldsymbol{x}_4 = \lambda\boldsymbol{x}_4 \\ \mathbf{C}_c^{\mathcal{C}}\boldsymbol{x}_4 = \mathbf{0} \end{cases} \tag{27}$$

As $\boldsymbol{X}$ is non zero, it implies that $\boldsymbol{x}_4$ is non zero since $\boldsymbol{x}_1$, $\boldsymbol{x}_2$, $\boldsymbol{x}_3$ and $\boldsymbol{x}_5$ are zero vectors. Consequently, λ is an unobservable mode of $(\mathbf{A}_c^{\mathcal{C}}, \mathbf{C}_c^{\mathcal{C}})$. Conversely, if λ is an unobservable mode of $(\mathbf{A}_c^{\mathcal{C}}, \mathbf{C}_c^{\mathcal{C}})$, it is sufficient to consider $\boldsymbol{x}_1 = \mathbf{0}$, $\boldsymbol{x}_2 = \mathbf{0}$, $\boldsymbol{x}_3 = \mathbf{0}$, $\boldsymbol{x}_5 = \mathbf{0}$ and $\boldsymbol{x}_4 \neq \mathbf{0}$ such that

$\mathbf{A}_c^{\mathcal{C}}\boldsymbol{x}_4 = \lambda\boldsymbol{x}_4$ and $\mathbf{C}_c^{\mathcal{C}}\boldsymbol{x}_4 = \mathbf{0}$ to show that λ is an unobservable mode of $(\boldsymbol{\mathcal{A}}_a, \boldsymbol{\mathcal{C}}_a)$.

It remains now to show that λ is an unobservable mode of $(\mathbf{A}_c^{\mathcal{C}}, \mathbf{C}_c^{\mathcal{C}})$ if and only if it is an unobservable mode of $(\boldsymbol{\mathcal{A}}_l, \boldsymbol{\mathcal{C}}_l)$. We first consider the case $\lambda \neq 0$. If there exists a non zero vector $\boldsymbol{x}$ such that $\mathbf{A}_c^{\mathcal{C}}\boldsymbol{x} = \lambda\boldsymbol{x}$ and $\mathbf{C}_c^{\mathcal{C}}\boldsymbol{x} = \mathbf{0}$. Then $\boldsymbol{X} = [\mathbf{0}^\top \ \boldsymbol{x}^\top]^\top$ is a non zero vector such that $\boldsymbol{\mathcal{A}}_l\boldsymbol{X} = \lambda\boldsymbol{X}$ and $\boldsymbol{\mathcal{C}}_l\boldsymbol{X} = \mathbf{0}$. Conversely, assume that there exists a non zero vector $\boldsymbol{X} = [\boldsymbol{x}_1^\top \ \boldsymbol{x}_2^\top]^\top$ such that $\boldsymbol{\mathcal{A}}_l\boldsymbol{X} = \lambda\boldsymbol{X}$ and $\boldsymbol{\mathcal{C}}_l\boldsymbol{X} = \mathbf{0}$. The first equality implies $\lambda\boldsymbol{x}_1 = \mathbf{0}$. As $\lambda \neq 0$, we have $\boldsymbol{x}_1 = \mathbf{0}$, which yields $\boldsymbol{x}_2 \neq \mathbf{0}$, $\mathbf{A}_c^{\mathcal{C}}\boldsymbol{x}_2 = \lambda\boldsymbol{x}_2$ and $\mathbf{C}_c^{\mathcal{C}}\boldsymbol{x}_2 = \mathbf{0}$.

In the case $\lambda = 0$, $\boldsymbol{\mathcal{A}}_l\boldsymbol{X} = \lambda\boldsymbol{X} = \mathbf{0}$ and $\boldsymbol{\mathcal{C}}_l\boldsymbol{X} = \mathbf{0}$ imply:

$$\begin{bmatrix} \mathbf{A}_i^{\mathcal{C}} & \mathbf{A}_c^{\mathcal{C}} \\ \mathbf{C}_i^{\mathcal{C}} & \mathbf{C}_c^{\mathcal{C}} \end{bmatrix} \boldsymbol{X} = \mathbf{0}.$$

Based on (A1), we have $\boldsymbol{X} = \mathbf{0}$, and hence $\lambda = 0$ cannot be an unobservable mode of $(\boldsymbol{\mathcal{A}}_l, \boldsymbol{\mathcal{C}}_l)$. Similarly $\lambda = 0$ cannot be an unobservable mode of $(\mathbf{A}_c^{\mathcal{C}}, \mathbf{C}_c^{\mathcal{C}})$ since based on (A1), $\mathbf{A}_c^{\mathcal{C}}\boldsymbol{x} = \lambda\boldsymbol{x} = \mathbf{0}$ and $\mathbf{C}_c^{\mathcal{C}}\boldsymbol{x} = \mathbf{0}$ imply $\boldsymbol{x} = \mathbf{0}$. □

Lemma 2: *For any $\lambda \in \mathbb{R}_+^*$, λ is an uncontrollable mode of $(\boldsymbol{\mathcal{A}}_a, \boldsymbol{\mathcal{B}}_a)$ if and only if it is an uncontrollable mode of $(\boldsymbol{\mathcal{A}}_l, \boldsymbol{\mathcal{B}}_l)$.*

Proof: Let $\boldsymbol{X} = \begin{bmatrix}\boldsymbol{x}_1^\top \ \boldsymbol{x}_2^\top \ \boldsymbol{x}_3^\top \ \boldsymbol{x}_4^\top \ \boldsymbol{x}_5^\top\end{bmatrix}^\top$ be a non zero vector with suitable dimensions such that $\boldsymbol{X}^\top\boldsymbol{\mathcal{A}}_a = \lambda\boldsymbol{X}^\top$ and $\boldsymbol{X}^\top\boldsymbol{\mathcal{B}}_a = \mathbf{0}$. After some algebra, it is equivalent to the following system:

$$\begin{cases} \begin{bmatrix} \frac{1}{\lambda}\boldsymbol{x}_4^\top\mathbf{A}_i^{\mathcal{C}} \,,\, \boldsymbol{x}_4^\top \end{bmatrix} \boldsymbol{\mathcal{A}}_l = \lambda \begin{bmatrix} \frac{1}{\lambda}\boldsymbol{x}_4^\top\mathbf{A}_i^{\mathcal{C}} \,,\, \boldsymbol{x}_4^\top \end{bmatrix} \\ \begin{bmatrix} \frac{1}{\lambda}\boldsymbol{x}_4^\top\mathbf{A}_i^{\mathcal{C}} \,,\, \boldsymbol{x}_4^\top \end{bmatrix} \boldsymbol{\mathcal{B}}_l = \mathbf{0} \\ \boldsymbol{x}_1^\top = \frac{\tau}{\lambda}\boldsymbol{x}_4^\top\mathbf{A}_i^{\mathcal{C}} \\ \boldsymbol{x}_2 = -\boldsymbol{x}_1 \\ \boldsymbol{x}_3 = \mathbf{0} \\ \boldsymbol{x}_5 = \mathbf{0} \end{cases} \tag{28}$$

To conclude that λ is an uncontrollable mode of $(\boldsymbol{\mathcal{A}}_l, \boldsymbol{\mathcal{B}}_l)$, it is sufficient to note that $\boldsymbol{X} \neq \mathbf{0}$ if and only if $\boldsymbol{x}_4 \neq \mathbf{0}$, i.e., if and only if $[1/\lambda\boldsymbol{x}_4^\top\mathbf{A}_i \,,\, \boldsymbol{x}_4^\top] \neq \mathbf{0}$. Conversely, let $\boldsymbol{Z} = \begin{bmatrix}\boldsymbol{z}_1^\top \ \boldsymbol{z}_2^\top\end{bmatrix}^\top$ be a non zero vector with suitable dimensions such that $\boldsymbol{Z}^\top\boldsymbol{\mathcal{A}}_l = \lambda\boldsymbol{Z}^\top$ and $\boldsymbol{Z}^\top\boldsymbol{\mathcal{B}}_l = \mathbf{0}$. The first equality implies that $\boldsymbol{z}_2^\top\mathbf{A}_i^{\mathcal{C}} = \lambda\boldsymbol{z}_1^\top$. Consequently, as $\lambda \neq 0$ and $\boldsymbol{Z}$ is a non zero vector, we have $\boldsymbol{z}_2 \neq \mathbf{0}$. Therefore, with $\boldsymbol{x}_4 = \boldsymbol{z}_2$, it sufficient to consider $\boldsymbol{x}_1$, $\boldsymbol{x}_2$, $\boldsymbol{x}_3$ and $\boldsymbol{x}_5$ as defined by (28) to conclude that λ is an uncontrollable mode of $(\boldsymbol{\mathcal{A}}_a, \boldsymbol{\mathcal{B}}_a)$. □

Lemma 3: *Assume that (A1) and (A2) hold. Then a zero-valued λ cannot be an uncontrollable mode of $(\boldsymbol{\mathcal{A}}_a, \boldsymbol{\mathcal{B}}_a)$, neither $(\boldsymbol{\mathcal{A}}_l, \boldsymbol{\mathcal{B}}_l)$.*

Proof: Let $\boldsymbol{X} = \begin{bmatrix}\boldsymbol{x}_1^\top \ \boldsymbol{x}_2^\top \ \boldsymbol{x}_3^\top \ \boldsymbol{x}_4^\top \ \boldsymbol{x}_5^\top\end{bmatrix}^\top$ be a vector with suitable dimensions such that $\boldsymbol{X}^\top\boldsymbol{\mathcal{A}}_a = \mathbf{0}$

and $\boldsymbol{X}^\top \boldsymbol{\mathcal{B}}_a = \mathbf{0}$. After some algebra, it is equivalent to the following system:

$$\begin{cases} \mathbf{0} = [\tau \boldsymbol{x}_4^\top \,,\, \boldsymbol{x}_5^\top] \begin{bmatrix} \mathbf{A}_c^{\mathcal{C}} & \mathbf{A}_i^{\mathcal{C}} \\ \mathbf{C}_c^{\mathcal{C}} & \mathbf{C}_i^{\mathcal{C}} \end{bmatrix} \\ \boldsymbol{x}_1^\top = -\tau \boldsymbol{x}_4^\top \mathbf{B}_r^{\mathcal{C}} - \boldsymbol{x}_5^\top \mathbf{D}_r^{\mathcal{C}} \\ \boldsymbol{x}_2^\top = -\tau \boldsymbol{x}_4^\top \mathbf{B}_1^{\mathcal{C}} - \boldsymbol{x}_5^\top \mathbf{D}_1^{\mathcal{C}} \\ \boldsymbol{x}_3^\top = -\tau \boldsymbol{x}_4^\top \mathbf{B}_2^{\mathcal{C}} - \boldsymbol{x}_5^\top \mathbf{D}_2^{\mathcal{C}} \end{cases} \tag{29}$$

Based on assumptions (A1) and (A2), matrix (15) is square and full column rank, and hence, it is invertible. Consequently, system (29) is equivalent to $\boldsymbol{X} = \mathbf{0}$.

Now, let $\boldsymbol{X} = \left[\boldsymbol{x}_1^\top \ \boldsymbol{x}_2^\top\right]^\top$ be a vector with suitable dimensions such that $\boldsymbol{X}^\top \boldsymbol{\mathcal{A}}_l = \mathbf{0}$ and $\boldsymbol{X}^\top \boldsymbol{\mathcal{B}}_l = \mathbf{0}$. Then, $\boldsymbol{X}^\top \boldsymbol{\mathcal{A}}_l = \mathbf{0}$ implies:

$$\left[\boldsymbol{x}_2^\top, \mathbf{0}^\top\right] \begin{bmatrix} \mathbf{A}_c^{\mathcal{C}} & \mathbf{A}_i^{\mathcal{C}} \\ \mathbf{C}_c^{\mathcal{C}} & \mathbf{C}_i^{\mathcal{C}} \end{bmatrix} = \mathbf{0}$$

Since matrix (15) is invertible, $\boldsymbol{x}_2 = \mathbf{0}$. Furthermore, as $\boldsymbol{X}^\top \boldsymbol{\mathcal{B}}_l = \mathbf{0}$ implies $\boldsymbol{x}_1^\top + \boldsymbol{x}_2^\top \mathbf{B}_r^{\mathcal{C}} = \mathbf{0}$, we conclude that $\boldsymbol{x}_1 = \mathbf{0}$ and then $\boldsymbol{X} = \mathbf{0}$. □

We can now introduce the following main result.

Theorem 2: *Assume that (A1), (A2) and (A3) hold. Then, $(\boldsymbol{\mathcal{A}}_a, \boldsymbol{\mathcal{B}}_a, \boldsymbol{\mathcal{C}}_a, \boldsymbol{\mathcal{D}}_a)$ is stabilizable and detectable. Furthermore, assume that $\mathcal{CL}(\mathcal{S}_l(\boldsymbol{\theta}_e), \mathcal{C}_l(\boldsymbol{\theta}_e))$ is internally stable, then so is $\mathcal{CL}_l(\mathcal{S}, \mathcal{C})(\boldsymbol{\theta}_e)$.*

Proof: Based on Lemmas 1, 2 and 3, it is straightforward to conclude that $(\boldsymbol{\mathcal{A}}_a, \boldsymbol{\mathcal{B}}_a, \boldsymbol{\mathcal{C}}_a, \boldsymbol{\mathcal{D}}_a)$ is stabilizable and detectable since (A3) assumes that $(\boldsymbol{\mathcal{A}}_l, \boldsymbol{\mathcal{B}}_l, \boldsymbol{\mathcal{C}}_l, \boldsymbol{\mathcal{D}}_l)$ is stabilizable and detectable. Furthermore, if we assume that $\mathcal{CL}(\mathcal{S}_l(\boldsymbol{\theta}_e), \mathcal{C}_l(\boldsymbol{\theta}_e))$ is internally stable, we can directly conclude that $\mathcal{CL}_l(\mathcal{S}, \mathcal{C})(\boldsymbol{\theta}_e)$ is internally stable since the internal stability property does not depend on specific stabilizable and detectable state-space representations of the plant and the controller (Zhou, Doyle, & Glover, 1996). □

Theorems 1 and 2 show that the filtering parameter $\tau > 0$ has no impact on the controller transfer function and the internal stability of the closed-loop system. Consequently, τ can be tuned based on the behaviour of the nonlinear closed-loop system $\mathcal{CL}(\mathcal{S}, \mathcal{C})$. This is a fundamental difference from the classic velocity-based implementation using pseudo-derivative. Furthermore, we have demonstrated that a nonlinear gain-scheduled controller $\mathcal{C}$ solving Problem 1 can always be found. Therefore, assuming that the set of LTI controllers $\mathcal{C}_l$ has been designed such that for any operating point $\boldsymbol{\theta}_e \in \Theta$, $\mathcal{CL}(\mathcal{S}_l(\boldsymbol{\theta}_e), \mathcal{C}_l(\boldsymbol{\theta}_e))$ is internally stable, the stability of the resulting closed-loop nonlinear system $\mathcal{CL}(\mathcal{S}, \mathcal{C})$ is guaranteed for slow time variations of the reference input $\boldsymbol{r}$ and the exogenous input $\boldsymbol{w}$ (Lawrence, D., & Rugh, 1990; Rugh, & Shamma, 2000).

3.2.3 Selection of the pre/post-filtering strategy

In this subsection, we investigate what kind of pre/post-filtering can be used in the enhanced velocity-based implementation so that Theorems 1 and 2 hold.

Based on Fig. 5, we are looking for scalar rational transfer functions $F_r(s)$, $F_{y_1}(s)$, $F_{y_2}(s)$ and $F_v(s)$ such that the gain-scheduled controller $\tilde{\mathcal{C}}$ given by (30) solves Problem 1. In this setting, the parameter $\tau \in \mathbb{R}^*$ is still a scaling factor for both $\mathbf{A}_i^{\mathcal{C}}(\boldsymbol{\theta})$ and $\mathbf{C}_i^{\mathcal{C}}(\boldsymbol{\theta})$, and

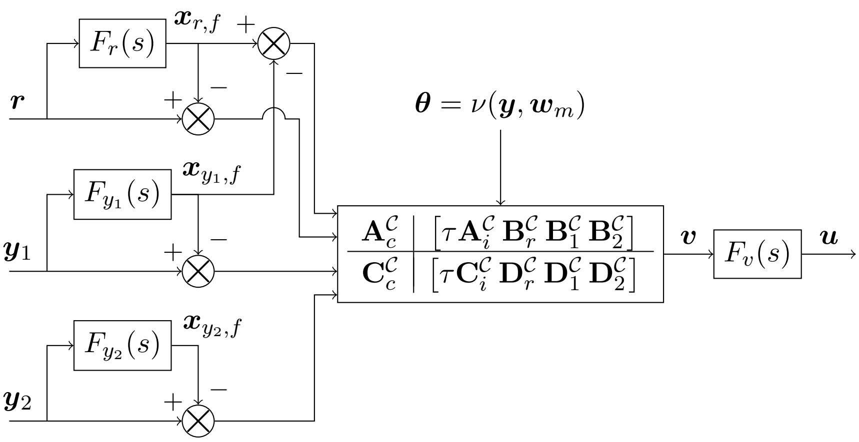

Figure 5. Enhanced velocity-based implementation: pre/post-filtering strategy

$$
\tilde{\mathcal{C}} := \begin{cases}
\boldsymbol{x}_{r,f} = F_r(s)\boldsymbol{r} \\
\boldsymbol{x}_{y_1,f} = F_{y_1}(s)\boldsymbol{y}_1 \\
\boldsymbol{x}_{y_2,f} = F_{y_2}(s)\boldsymbol{y}_2 \\
\dot{\boldsymbol{x}}_c = \mathbf{A}_c^{\mathcal{C}}(\boldsymbol{\theta})\boldsymbol{x}_c + \tau\mathbf{A}_i^{\mathcal{C}}(\boldsymbol{\theta})[\boldsymbol{x}_{r,f} - \boldsymbol{x}_{y_1,f}] \\
\qquad + \mathbf{B}_r^{\mathcal{C}}(\boldsymbol{\theta})[\boldsymbol{r} - \boldsymbol{x}_{r,f}] + \mathbf{B}_1^{\mathcal{C}}(\boldsymbol{\theta})[\boldsymbol{y}_1 - \boldsymbol{x}_{y_1,f}] + \mathbf{B}_2^{\mathcal{C}}(\boldsymbol{\theta})[\boldsymbol{y}_2 - \boldsymbol{x}_{y_2,f}] \\
\boldsymbol{v} = \mathbf{C}_c^{\mathcal{C}}(\boldsymbol{\theta})\boldsymbol{x}_c + \tau\mathbf{C}_i^{\mathcal{C}}(\boldsymbol{\theta})[\boldsymbol{x}_{r,f} - \boldsymbol{x}_{y_1,f}] \\
\qquad + \mathbf{D}_r^{\mathcal{C}}(\boldsymbol{\theta})[\boldsymbol{r} - \boldsymbol{x}_{r,f}] + \mathbf{D}_1^{\mathcal{C}}(\boldsymbol{\theta})[\boldsymbol{y}_1 - \boldsymbol{x}_{y_1,f}] + \mathbf{D}_2^{\mathcal{C}}(\boldsymbol{\theta})[\boldsymbol{y}_2 - \boldsymbol{x}_{y_2,f}] \\
\boldsymbol{u} = F_v(s)\boldsymbol{v} \\
\boldsymbol{\theta} = \nu(\boldsymbol{y}, \boldsymbol{w}_m)
\end{cases} \tag{30}
$$

Analyzing the proof of Theorem 1, the key point enabling to avoid the emergence of the hidden coupling terms in the linearized dynamics of the gain-scheduled controller lies in the trim conditions (16). Indeed, if these trim conditions are not satisfied, (19) and (20) cannot be simplified, leading to the occurrence of the hidden coupling terms. Therefore, to avoid the emergence of these terms when linearizing the gain-scheduled controller $\tilde{\mathcal{C}}$, the trim conditions must satisfy: $\boldsymbol{x}_{r,f,e} = \boldsymbol{r}_e$, $\boldsymbol{x}_{y_1,f,e} = \boldsymbol{y}_{1,e}$, $\boldsymbol{x}_{y_2,f,e} = \boldsymbol{y}_{2,e}$ and $\boldsymbol{v}_e = 0$. In this case, based on Assumption (A1) and equation (17), it will imply the two remaining key constraints $\boldsymbol{r}_e = \boldsymbol{y}_{1,e}$ and $\boldsymbol{x}_{c,e} = \mathbf{0}$. The condition $\boldsymbol{x}_{r,f,e} = \boldsymbol{r}_e$, as $\boldsymbol{x}_{r,f} = F_r(s)\boldsymbol{r}$, is equivalent to $F_r(0) = 1$. Similarly, we have $F_{y_1}(0) = F_{y_2}(0) = 1$. Finally, to impose $\boldsymbol{v}_e = 0$, as $\boldsymbol{u} = F_v(s)\boldsymbol{v}$, $F_v(s)$ must contain an integral component, i.e., $F_v(s) = F_v^*(s)/s$ with $F_v^*(s)$ a rational transfer function such that $F_v^*(0) \neq 0$. Under these conditions, as they prevent the emergence of the hidden coupling terms, a direct computation, similar to the one achieved in the proof of Theorem 1, shows that:

$$
\begin{aligned}
\boldsymbol{\Delta u}(s) =& \tau F_v(s)\left[\mathbf{C}_i^{\mathcal{C}}(\boldsymbol{\theta}_e) + \mathbf{C}_c^{\mathcal{C}}(\boldsymbol{\theta}_e)(s\mathbf{I}_n - \mathbf{A}_c^{\mathcal{C}}(\boldsymbol{\theta}_e))^{-1}\mathbf{A}_i^{\mathcal{C}}(\boldsymbol{\theta}_e)\right](F_r(s)\boldsymbol{\Delta r}(s) - F_{y_1}(s)\boldsymbol{\Delta y}_1(s)) \\
&+ F_v(s)(1 - F_r(s))\left[\mathbf{D}_r^{\mathcal{C}}(\boldsymbol{\theta}_e) + \mathbf{C}_c^{\mathcal{C}}(\boldsymbol{\theta}_e)(s\mathbf{I}_n - \mathbf{A}_c^{\mathcal{C}}(\boldsymbol{\theta}_e))^{-1}\mathbf{B}_r^{\mathcal{C}}(\boldsymbol{\theta}_e)\right]\boldsymbol{\Delta r}(s) \\
&+ F_v(s)(1 - F_{y_1}(s))\left[\mathbf{D}_1^{\mathcal{C}}(\boldsymbol{\theta}_e) + \mathbf{C}_c^{\mathcal{C}}(\boldsymbol{\theta}_e)(s\mathbf{I}_n - \mathbf{A}_c^{\mathcal{C}}(\boldsymbol{\theta}_e))^{-1}\mathbf{B}_1^{\mathcal{C}}(\boldsymbol{\theta}_e)\right]\boldsymbol{\Delta y}_1(s) \\
&+ F_v(s)(1 - F_{y_2}(s))\left[\mathbf{D}_2^{\mathcal{C}}(\boldsymbol{\theta}_e) + \mathbf{C}_c^{\mathcal{C}}(\boldsymbol{\theta}_e)(s\mathbf{I}_n - \mathbf{A}_c^{\mathcal{C}}(\boldsymbol{\theta}_e))^{-1}\mathbf{B}_2^{\mathcal{C}}(\boldsymbol{\theta}_e)\right]\boldsymbol{\Delta y}_2(s)
\end{aligned} \tag{31}
$$

The objective is then to select the pre/post filtering transfer functions such that (31) coincides with the linear controller dynamics $\mathcal{C}_l(\boldsymbol{\theta}_e)$ given in (23). [Reviewer 1 - Remark 3] As we are looking for a generic scheme, this equality must hold for any matrices $\mathbf{A}_c^{\mathcal{C}}(\boldsymbol{\theta}_e), \ldots, \mathbf{D}_2^{\mathcal{C}}(\boldsymbol{\theta}_e)$ with suitable dimensions. It allows in the subsequent developments considering specific values of these matrices in order to derive the properties of the desired filters.

Taking $\boldsymbol{\Delta r}(s) = \boldsymbol{\Delta y}_1(s) = \mathbf{0}$, since the equality between (31) and (23) must hold for any $\boldsymbol{\Delta y}_2(s)$, we have

$$[F_v(s)(1 - F_{y_2}(s)) - 1] \left[\mathbf{D}_2^{\mathcal{C}}(\boldsymbol{\theta}_e) + \mathbf{C}_c^{\mathcal{C}}(\boldsymbol{\theta}_e)(s\mathbf{I}_n - \mathbf{A}_c^{\mathcal{C}}(\boldsymbol{\theta}_e))^{-1}\mathbf{B}_2^{\mathcal{C}}(\boldsymbol{\theta}_e)\right] = \mathbf{0}.$$

[Reviewer 1 - Remark 3] Again, as we aim at finding a generic implementation, this equality must hold for any matrices $\mathbf{A}_c^{\mathcal{C}}(\boldsymbol{\theta}_e), \ldots, \mathbf{D}_2^{\mathcal{C}}(\boldsymbol{\theta}_e)$ with suitable dimensions. In particular, it must hold for $\mathbf{C}_c^{\mathcal{C}}(\boldsymbol{\theta}_e) = \mathbf{0}$ and a non zero matrix $\mathbf{D}_c^{\mathcal{C}}(\boldsymbol{\theta}_e)$. Thus, we deduce that

$$F_v(s)(1 - F_{y_2}(s)) = 1. \tag{32}$$

Then, considering the equality between (23) and (31) while taking $\boldsymbol{\Delta y}_2(s) = \mathbf{0}$, $\boldsymbol{\Delta r}(s) = \boldsymbol{\Delta y}_1(s)$ and $\mathbf{C}_c^{\mathcal{C}}(\boldsymbol{\theta}_e) = \mathbf{0}$, it yields

$$[F_v(s)(1 - F_r(s)) - 1]\, \mathbf{D}_r^{\mathcal{C}}(\boldsymbol{\theta}_e) + [F_v(s)(1 - F_{y_1}(s)) - 1]\, \mathbf{D}_1^{\mathcal{C}}(\boldsymbol{\theta}_e) = \mathbf{0}.$$

In particular, choosing $\mathbf{D}_r^{\mathcal{C}}(\boldsymbol{\theta}_e) = \mathbf{I}_{p_1}$ and $\mathbf{D}_{y_1}^{\mathcal{C}}(\boldsymbol{\theta}_e) = \mathbf{0}$, the last matrix equality boils down to

$$F_v(s)(1 - F_r(s)) = 1. \tag{33}$$

Conversely, choosing $\mathbf{D}_r^{\mathcal{C}}(\boldsymbol{\theta}_e) = \mathbf{0}$ and $\mathbf{D}_{y_1}^{\mathcal{C}}(\boldsymbol{\theta}_e) = \mathbf{I}_{p_1}$ we have

$$F_v(s)(1 - F_{y_1}(s)) = 1. \tag{34}$$

Thus, based on (32-34),

$$F_r(s) = F_{y_1}(s) = F_{y_2}(s) = 1 - \frac{1}{F_v(s)}. \tag{35}$$

Finally, considering again the equality between (23) and (31) while taking $\boldsymbol{\Delta y}_2(s) = \mathbf{0}$, $\boldsymbol{\Delta y}_1(s) = -\boldsymbol{\Delta r}(s)$ and $\mathbf{C}_c^{\mathcal{C}}(\boldsymbol{\theta}_e) = \mathbf{0}$, we have, based on (35),

$$\left[\tau F_v(s) F_r(s) - \frac{1}{s}\right] \mathbf{C}_i^{\mathcal{C}}(\boldsymbol{\theta}_e) = \mathbf{0}.$$

Moreover, as this matrix equality must hold for any matrix $\mathbf{C}_i^{\mathcal{C}}(\boldsymbol{\theta}_e)$ with suitable dimensions, we have

$$\tau F_v(s) F_r(s) = \frac{1}{s}. \tag{36}$$

Combining (35) and (36), simple algebra yields $F_r(s) = F_{y_1}(s) = F_{y_2}(s) = 1/(\tau s + 1)$ and $F_v(s) = 1 + 1/(\tau s)$. Obviously, these results are compatible with the trim conditions formerly established, i.e., $F_r(0) = F_{y_1}(0) = F_{y_2}(0) = 1$ and $F_v(s)$ presents an integral component. Consequently, the filters proposed in the enhanced velocity-based implementation (14) are the only possible choice for which Theorem 1 holds.

4. Case study

In the following, we illustrate the approach proposed in this paper through the implementation of a pitch-axis missile autopilot.

4.1 *Missile Nonlinear Model and Self-Scheduled Controller*

4.1.1 Nonlinear Model

The considered pitch-axis model of the missile involving the angle of attack α and the pith rate q is the one given by (Reichert, 1992):

$$\begin{cases} \dot{\alpha} = K_\alpha M C_n\left(\alpha, \delta, M\right)\cos(\alpha) + q \\ \dot{q} = K_q M^2 C_m\left(\alpha, \delta, M\right) \end{cases} \tag{37}$$

where $C_n\left(\alpha, \delta, M\right)$ and $C_m\left(\alpha, \delta, M\right)$ are respectively the lift and the pitching-moment aerodynamic coefficients. The dynamics of the actual tail deflection δ related to the commanded tail deflection u are modelled by a second order system. The system output is the normal acceleration η given by:

$$\eta = K_z M^2 C_n\left(\alpha, \delta, M\right). \tag{38}$$

The measured outputs available for feedback are η and q. The angle of attack α (an endogenous variable) and the Mach number M (an exogenous variable) are used as scheduling parameters. The plant input is the commanded tail deflection δ_c. Further description of the physical parameters involved in the model, including their numerical values, are given in (Reichert, 1992).

4.1.2 Gain-Scheduled Controller Design

The control objective is to design an autopilot allowing to track commanded normal accelerations η_c over the flight domain $M \in [2, 4]$ and $\alpha \in [-20^\circ, 20^\circ]$. Among other possibilities, this design can be achieved via a self-scheduling approach based on eigenstructure assignment techniques (Le Gorrec, Magni, Carsten, & Chiappa, 1998). Such a procedure has been applied in (Döll, Le Gorrec, Ferreres, & Magni, 2001) for the following set of LTI controllers parametrized by the operating point $\boldsymbol{\theta}_e = (\alpha_e, M_e)$:

$$\begin{cases} \delta\dot{x}_i = \delta\eta_c - \delta\eta \\ \delta u = K_i(\boldsymbol{\theta}_e)\delta x_i + K_\eta(\boldsymbol{\theta}_e)\delta\eta + K_q(\boldsymbol{\theta}_e)\delta q \end{cases} \tag{39}$$

where K_i, K_η and K_q are quadratic functions of the flight condition $\boldsymbol{\theta}_e$. The scheduled gains have been tuned based on the six operating points and associated eigenvalue assignment of Tab. 1. Their numerical values are given in (Döll, Le Gorrec, Ferreres, & Magni, 2001).

4.2 *Gain-scheduled controller implementation*

This subsection presents the results and the comparison of the performance of the naive, the velocity-based and the enhanced velocity-based implementations.

Table 1. Operating points and associated eigenvalue assignment considered in the synthesis

M_e	α_e	λ_r	λ_c
4	20 deg	-14	$-19 \pm 19j$
4	0 deg	-13.9	$-15 \pm 16j$
2	0 deg	-12	$-12 \pm 12j$
2	20 deg	-13.5	$-13.5 \pm 13.5j$
4	10 deg	-13.7	$-13.7 \pm 13.7j$
3	0 deg	-12.5	No constraint

4.2.1 Naive implementation

The naive implementation has a structure similar to that of the LTI controllers used for design purposes:

$$\mathcal{C}_{\text{naive}} := \begin{cases} \dot{x}_i = \eta_c - \eta \\ u = K_i(\alpha, M)x_i + K_\eta(\alpha, M)\eta + K_q(\alpha, M)q \end{cases}$$

However, as scheduled gains are varying according to the state signal α, the linearization of $\mathcal{C}_{\text{naive}}$ at a given operating point $\boldsymbol{\theta}_e$ brings hidden coupling terms that are not present in (39). For instance, at the operating point $M_e = 4$ and $\alpha_e = 10\,\text{deg}$, the assigned poles are located at -13.7 and $-13.7 \pm 13.7j$. Nevertheless, with the naive implementation, the actual pole location is very different, i.e., -47.9 and $-1.49 \pm 10.6j$. Particularly, the complex pair exhibits a very low damping, leading to large overshoots.

4.2.2 Velocity-based implementation

As the measurement of $\dot{\eta}$ and $\dot{q}$ is not available for feedback, the velocity-based implementation is achieved via the pseudo derivative of the normal acceleration η and the pitch-rate q with a constant $\tau > 0$:

$$\mathcal{C}_{\text{vel}} := \begin{cases} \dot{\eta}_f = \tau^{-1}\eta_f - \tau^{-1}\eta \\ \dot{q}_f = \tau^{-1}q_f - \tau^{-1}q \\ v = \tau K_i(\alpha, M)(\eta_c - \eta) + K_\eta(\alpha, M)(\eta - \eta_f) + K_q(\alpha, M)(q - q_f) \\ \dot{u} = \tau^{-1}v \end{cases}$$

As mentioned previously, the pseudo derivative introduces an extra dynamic component in the controller, which is not considered in the design.

4.2.3 Enhanced velocity-based implementation

The enhanced velocity-based implementation, denoted $\mathcal{C}_{\text{vel+}}$, is of the following form for $\tau > 0$:

$$\mathcal{C}_{\text{vel+}} := \begin{cases} \dot{\eta}_{c,f} = \tau^{-1}\eta_{c,f} - \tau^{-1}\eta_c \\ \dot{\eta}_f = \tau^{-1}\eta_f - \tau^{-1}\eta \\ \dot{q}_f = \tau^{-1}q_f - \tau^{-1}q \\ v = \tau K_i(\alpha, M)(\eta_{c,f} - \eta_f) + K_\eta(\alpha, M)(\eta - \eta_f) + K_q(\alpha, M)(q - q_f) \\ \dot{x}_{v,f} = \tau^{-1}v \\ u = x_{v,f} + v \end{cases}$$

Assuming that $K_i(\alpha, M) \neq 0$ over the operating domain, Theorems 1 and 2 guarantee that $\mathcal{C}_{\text{vel+}}$ is a safe implementation of the designed gain-scheduled controller.

4.3 *Nonlinear simulations*

The temporal behaviour of the three closed-loop systems with nonlinear controllers $\mathcal{C}_{\text{naive}}$, $\mathcal{C}_{\text{vel}}$ and $\mathcal{C}_{\text{vel+}}$, is simulated for a realistic profile of the Mach number (Reichert, 1992):

$$\begin{cases} \dot{M} = \dfrac{1}{v_s}\left(-|\eta| g \sin(|\alpha|) + A_x M^2 \cos(\alpha)\right) \\ M(0) = 3.0 \end{cases}$$

Simulation results are depicted in Figs. 6 and 7. Note that the open-loop pitch-axis missile benchmark model, when the normal acceleration η is selected as the output, exhibits unstable zeros resulting in an initial undershoot in their step-responses. As predicted for the naive implementation $\mathcal{C}_{naive}$, the hidden coupling terms interfere in the closed-loop dynamics, leading to large overshoots for important command inputs. On the contrary, Fig. 6(a) shows that both velocity-based $\mathcal{C}_{vel}$ and enhanced velocity-based $\mathcal{C}_{vel+}$ implementations work well with a similar behaviour for sufficiently small filtering parameters, e.g., $\tau = 0.002$. The evolution of the Mach number, which is the exogenous scheduling variable, is depicted in Fig. 6(b). Nevertheless, small values of τ may not be suitable in practice particularly due to measurement noises in the closed-loop system. As illustrated, for higher values of the filtering parameters, e.g., $\tau = 0.02$ (see Fig. 7), the closed-loop system performance of the velocity-based implementation $\mathcal{C}_{vel}$ is significantly degraded due to the interference of the pole introduced by the pseudo-derivative scheme. In sharp contrast, the enhanced velocity-base implementation $\mathcal{C}_{vel+}$ is mostly insensitive to the variation of the filtering parameter τ.

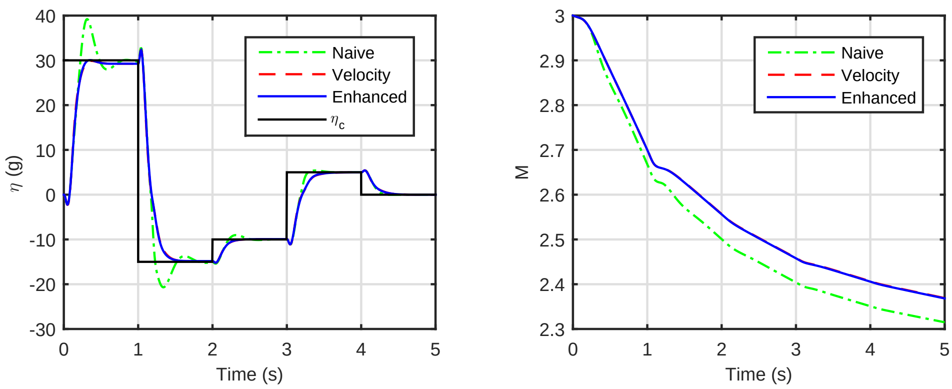

(a) Normal acceleration

(b) Mach number

Figure 6. Comparison of the closed-loop response to a series of step commands in acceleration - $\tau = 0.002$

Finally, the impact of the choice of the filtering parameter on the system in closed loop when white noise is introduced in the feedback loop by the measurement of both system outputs and scheduling variables is illustrated in Figs. 8 and 9. [Reviewer 1 - Remark 4] As expected, as both implementations are based on a pseudo-derivation scheme employing the transfer function $s/(\tau s + 1)$, a small value of the parameter τ will induce noise amplification, which may significantly degrade the performance of the closed-loop system for both strategies. Thus, an arbitrary small value of the filtering parameter τ is not appropriate for practical applications. However, in accordance with the conclusions of the above analysis, a larger value of the pseudo-derivative parameter also degrades the performance of the closed-loop system for the velocity-based implementation $\mathcal{C}_{\text{vel}}$ (see Fig. 8).

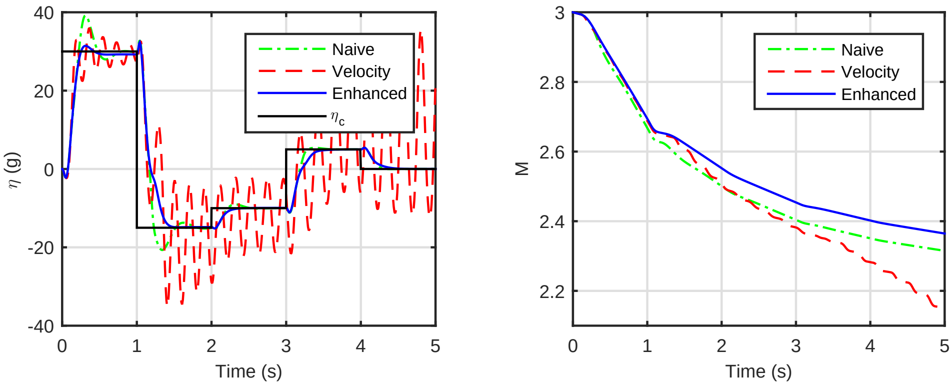

(a) Normal acceleration (b) Mach number

Figure 7. Comparison of the closed-loop to a series of step commands in acceleration - $\tau = 0.02$

Conversely, the enhanced velocity-based implementation $\mathcal{C}_{\text{vel}+}$ allows much higher values of the filtering parameter τ. Consequently, it results in an improved closed-loop performance, even in the presence of noise in the feedback loop (see Fig. 9).

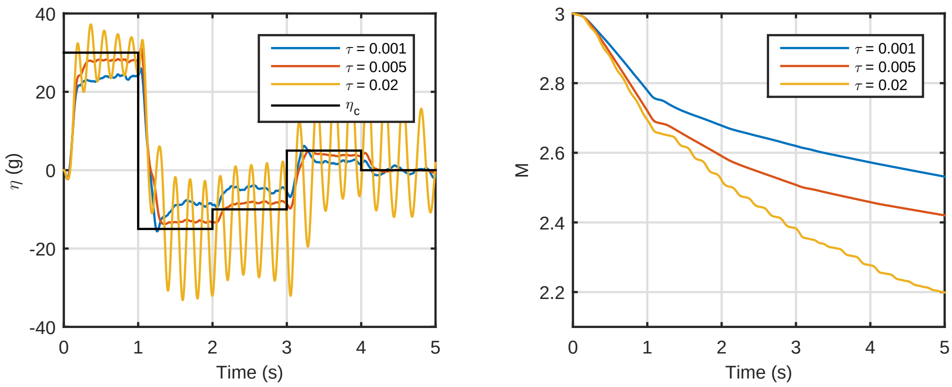

(a) Normal acceleration (b) Mach number

Figure 8. Closed-loop response for the velocity-based implementation $\mathcal{C}_{\text{vel}}$ in the presence of white noise in the feedback loop

5. Conclusion

This paper introduced an enhanced velocity-based algorithm for safe implementation of gain-scheduled controllers. Based on a parameter dependent set of LTI controllers that are designed to ensure the stability and performance of the linear closed-loop system for any frozen operating point, the proposed gain-scheduled controller implementation preserves both internal stability and input-output properties of the linearized closed-loop system. Furthermore, this implementation is relatively simple, with a gain-scheduled controller presenting an architecture similar to that of the original controller. The efficiency of the proposed approach has been demonstrated on the implementation of a pitch-axis missile autopilot. The simulation results confirmed the performance of the control system using the proposed new approach predicted by theoretical analysis.

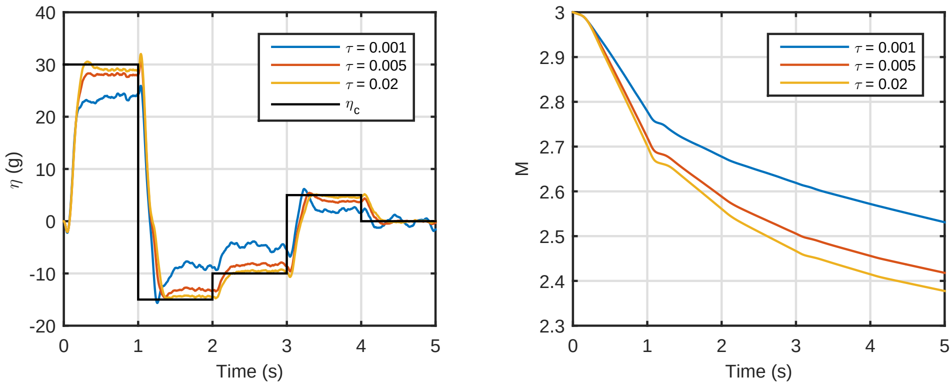

(a) $\mathcal{C}_{\mathrm{vel+}}$ - Normal acceleration

(b) $\mathcal{C}_{\mathrm{vel+}}$ - Mach number

Figure 9. Closed-loop response for the enhanced velocity-based implementation $\mathcal{C}_{\mathrm{vel+}}$ in the presence of white noise in the feedback loop

Acknowledgments

The authors would like to thank the Editor-in-Chief, the Associate Editor, and the anonymous reviewers for their constructive comments, which helped improve the quality of this paper.

References

Biannic, J. M., & Apkarian, P. (1999). Missile autopilot design via a modified LPV synthesis technique. *Aerospace Science and Technology*, 3(3), 153-1160.

Do Valle, R. C., Menegaldo, L. L., & Simões, A. M. (2014). Smoothly Gain-Scheduled Control of a Tri-Turbofan Airship. *Journal of Guidance, Control, and Dynamics*, 38(1), 53-61.

Döll, C., Le Gorrec, Y., Ferreres, G., & Magni, J.-F. (2001). A robust self-scheduled missile autopilot: design by multi-model eigenstructure assignment. *Control Engineering Practice*, 9(10), 1067-1078.

Kaminer, I., Pascoal, A. M, Khargonekar, P. P., & Coleman, E. E. (1995). A velocity algorithm for the implementation of gain-scheduled controllers. *Automatica*, 31(8), 1185-1191.

Khalil, H. K., & Grizzle, J. W. (1996). *Nonlinear systems*. Prentice hall New Jersey.

Lawrence, D., & Rugh, W. J. (1990). On a stability theorem for nonlinear systems with slowly varying inputs. *Automatic Control, IEEE Transactions on*, 35(7), 860-864.

Lawrence, D. A., & Rugh, W. J. (1995). Gain scheduling dynamic linear controllers for a nonlinear plant. *Automatica*, 31(3), 381-390.

Leith, D. J, & Leithead, W. E. (1998). Appropriate realisation of MIMO gain-scheduled controllers. *International journal of control*, 70(1), 13-50.

Leith, D. J (1999). Input-output linearization by velocity-based gain-scheduling. *International journal of control*, 72(3), 229-246.

Leith, D. J, & Leithead, W. E. (2000). Survey of gain-scheduling analysis and design. *International journal of control*, 73(11), 1001-1025.

Leith, D. J. and Leithead, W. E. (2000). Counter-example to a common LPV gain-scheduling design approach. *Proceedings of the UKACC International Control Conference.*

Le Gorrec, Y., Magni, J.-F., Carsten, D., & Chiappa, C. (1998). Modal multimodel control design approach applied to aircraft autopilot design. *Journal of guidance, control, and dynamics*, 21(1), 77-83.

Lhachemi, H., Saussié, D., & Zhu, G (2015). A structured H_∞-based optimization approach for integrated plant and self-scheduled flight control system design. *Aerospace Science and Technology*, 45, 30-38.

Lhachemi, H., Saussié, D., & Zhu, G (2016). Handling Hidden Coupling Terms in Gain-Sheduling Control Design: Application to a Pitch-Axis Missile Autopilot. *AIAA Scitech Guidance Naviguation and Control Conference.*

Lhachemi, H., Saussié, D., & Zhu, G (2016). Gain-Scheduling Control Design in the Presence of Hidden Coupling Terms. *Journal of Guidance, Control, and Dynamics*, Vol. 39, No. 8 (2016), pp. 1872-1880.

Lhachemi, H., Saussié, D., & Zhu, G (2016). Gain-scheduling control design in the presence of hidden coupling terms via eigenstructure assignment: Application to a pitch-axis missile autopilot. In *2016 American Control Conference (ACC)*, pp. 4041-4046. IEEE.

Magni, J.-F., Le Gorrec, Y., & Chiappa, C. (1998). A multimodel-based approach to robust and self-scheduled control design. *Decision and Control, 1998. Proceedings of the 37th IEEE Conference on*, 3, 3009-3014.

Naus, G. J. L. (2009). *Gain scheduling: Robust design and automated tuning of automotive controllers.* Ph.D. thesis, University of Technology Eindhoven.

Nichols, R., Reichert, R. T., & Rugh, W. J. (1993). Gain scheduling for H-infinity controllers: A flight control example. *Control Systems Technology, IEEE Transactions on*, 1(2), 69-79.

Reichert, R. T. (1992). Dynamic scheduling of modern-robust-control autopilot designs for missiles. *Control Systems, IEEE*, 12(5), 35-42.

Rugh, W. J. (1991). Analytical framework for gain scheduling. *Control Systems, IEEE*, 11(1), 79-84.

Rugh, W. J., & Shamma, J. S. (2000). Research on gain scheduling. *Automatica*, 36(10), 1401-1425.

Saussié, D., Saydy, L., & Akhrif, O. (2008). Gain scheduling control design for a pitch-axis missile autopilot. *AIAA Guidance, Navigation and Control Conference and Exhibit*, 7000.

Saussié, David, Saydy, L., Akhrif, O., & Bérard, C. (2011). Gain scheduling with guardian maps for longitudinal flight control. *Journal of Guidance, Control, and Dynamics*, 34(4), 1045-1059.

Shamma, J. S., & Athans, M. (1990). Analysis of gain scheduled control for nonlinear plants. *Automatic Control, IEEE Transactions on*, 35(8), 898-907.

Stilwell, D. J., & Rugh, W. J. (2000). Stability preserving interpolation methods for the synthesis of gain scheduled controllers. *Automatica*, 36(5), 665-671.

Vesel, V., & Ilka, A. (2013). Gain-scheduled PID controller design. *Journal of process control*, 23(8), 1141-1148.

Wu, F., Yang, X. H., Packard, A., & Becker, G. (1995). Induced L_2-norm control for LPV system with bounded parameter variation rates. *In American Control Conference, Proceedings of the 1995*, 3, 2379-2383.

Yang, W., Herrmann, G., Lowenberg, M., & Chen, X. (2010). Dynamic gain scheduled control in a multivariable control framework. *Decision and Control , 49th IEEE Conference on*, 7081-7086.

Yang, W., Hammoudi, N., Herrmann, G., Lowenberg, M., & Chen, X. (2012). Two-state dynamic gain scheduling control applied to an F16 aircraft model. *International Journal of Non-Linear Mechanics*, 47(10), 1116-1123.

Yang, W., Hammoudi, N., Herrmann, G., Lowenberg, M., & Chen, X. (2015). Dynamic gain-scheduled control and extended linearisation: extensions, explicit formulae and stability. *International Journal of Control*, 88(1), 163-179.

Zhou, K., Doyle, J. C., & Glover, K. (1996). *Robust and optimal control.* Prentice hall New Jersey.